

# Implementation of PCTides in NITES II: A Focus on Mean Lower Low Water Reference

**Jeffrey W. Book**  
Naval Research Laboratory

**Michael L. Incze**  
NUWC Division Newport



**Naval Undersea Warfare Center Division  
Newport, Rhode Island**

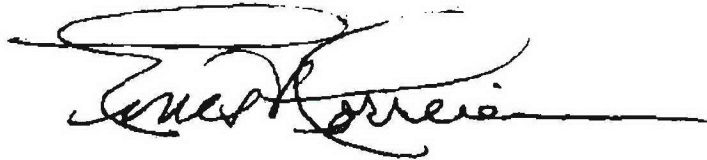
Approved for public release; distribution is unlimited.

## PREFACE

This document was prepared by the Naval Undersea Warfare Center (NUWC), Newport Division, and the Naval Research Laboratory (NRL), Oceanography Division, under the Naval Integrated Tactical Environmental System II (NITES II) development program. The supporting activities are the Space and Naval Warfare Systems Command and the NRL Advanced Graduate Research Program.

The authors wish to thank Ruth Preller, Pamela Posey, and David Walsh of NRL; Lisa Putallaz of Science Applications International Corporation; Art Najjar and Scott Cross of the Naval Oceanographic Office; and Maria Santos of NUWC Division Newport for their discussions and support during the analyses described in this document.

**Reviewed and Approved: 15 May 2006**



**Ernest Correia**  
**Head (*acting*), USW Combat Systems Department**



# REPORT DOCUMENTATION PAGE

*Form Approved*  
**OMB No. 0704-0188**

Public reporting for this collection of information is estimated to average 1 hour per response, including the time for reviewing instructions, searching existing data sources, gathering and maintaining the data needed, and completing and reviewing the collection of information. Send comments regarding this burden estimate or any other aspect of this collection of information, including suggestions for reducing this burden, to Washington Headquarters Services, Directorate for Information Operations and Reports, 1215 Jefferson Davis Highway, Suite 1204, Arlington, VA 22202-4302, and to the Office of Management and Budget, Paperwork Reduction Project (0704-0188), Washington, DC 20503.

<b>1. AGENCY USE ONLY (Leave blank)</b>	<b>2. REPORT DATE</b> 15 May 2006	<b>3. REPORT TYPE AND DATES COVERED</b>	
<b>4. TITLE AND SUBTITLE</b>  Implementation of PCTides in NITES II: A Focus on Mean Lower Low Water Reference		<b>5. FUNDING NUMBERS</b>  PR C458016	
<b>6. AUTHOR(S)</b>  Jeffrey W. Book, Michael L. Incze			
<b>7. PERFORMING ORGANIZATION NAME(S) AND ADDRESS(ES)</b>  Naval Undersea Warfare Center Division 1176 Howell Street Newport, RI 02841-1708		<b>8. PERFORMING ORGANIZATION REPORT NUMBER</b>  TD 11,745	
<b>9. SPONSORING/MONITORING AGENCY NAME(S) AND ADDRESS(ES)</b>  Space and Naval Warfare Systems Command 4301 Pacific Highway San Diego, CA 92110		<b>10. SPONSORING/MONITORING AGENCY REPORT NUMBER</b>  Naval Research Laboratory 4555 Overlook Avenue SW Washington, DC 20375	
<b>11. SUPPLEMENTARY NOTES</b>			
<b>12a. DISTRIBUTION/AVAILABILITY STATEMENT</b>  Approved for public release; distribution is unlimited.		<b>12b. DISTRIBUTION CODE</b>	
<b>13. ABSTRACT (Maximum 200 words)</b>  This document provides information concerning the implementation of the Naval Research Laboratory PCTides model in the Naval Integrated Tactical Environmental System (NITES) II for predicting the times and heights of sea surface levels and the speed and direction of tidal currents. The purpose is to provide guidance for model development and implementation upgrades that will better support tactical users of the NITES II software. Focus is placed on the representation of tidal heights with a reference to mean lower low water (MLLW), rather than the mean sea level (MSL) reference currently used in PCTides outputs. A complete algorithm has been developed to convert from an MSL reference to an MLLW reference using information available from the PCTides model. The algorithm is presented, and its performance is evaluated by comparing MLLW offsets from MSL calculated from simulated PCTides output with offsets more accurately determined from tidal coefficients. Additionally, a limited evaluation of the overall accuracy of the PCTides model is provided, and the implications for MLLW reference conversion are discussed. Recommendations for model development and a roadmap for improved implementation are presented.			
<b>14. SUBJECT TERMS</b>  Mean Lower Low Water (MLLW)      Oceanography      Tidal Currents Mean Sea Level (MSL)              PCTides Model      Tidal Heights NITES II			<b>15. NUMBER OF PAGES</b> 54
			<b>16. PRICE CODE</b>
<b>17. SECURITY CLASSIFICATION OF REPORT</b> Unclassified	<b>18. SECURITY CLASSIFICATION OF THIS PAGE</b> Unclassified	<b>19. SECURITY CLASSIFICATION OF ABSTRACT</b> Unclassified	<b>20. LIMITATION OF ABSTRACT</b> SAR

## TABLE OF CONTENTS

Section	Page
LIST OF ILLUSTRATIONS.....	ii
LIST OF TABLES .....	ii
LIST OF ABBREVIATIONS AND ACRONYMS .....	iii
1 INTRODUCTION.....	1
2 BACKGROUND.....	3
2.1 NITES II.....	3
2.1.1 NITES II Mission Focus .....	4
2.1.2 Coastal Predictions User Task.....	5
2.2 Tides Modeling .....	5
2.2.1 PCTides Model.....	5
2.2.2 MSL Versus MLLW .....	6
3 METHODOLOGY .....	9
3.1 Calculating MLLW Offsets from Tidal Coefficients.....	9
3.2 Test Regions and Databases.....	10
3.2.1 Developing an Algorithm Test Database and Simulating Algorithm Implementation .....	10
3.2.2 PCTides Runs and Measurement Datasets Used for Tidal Prediction Comparisons .....	11
3.3 Developing an Algorithm to Calculate PCTides MLLW Offsets .....	15
4 RESULTS AND ANALYSIS .....	17
4.1 Effectiveness of the PCTides MLLW Offset Algorithm .....	17
4.1.1 Simulated PCTides MLLW Offsets Compared wth Coefficient Calculated Offsets.....	18
4.1.2 Implementation of the MLLW Offset Algorithm in PCTides.....	19
4.2 Results from Limited Evaluations of PCTides SSH Accuracy .....	23
4.2.1 KTS Tidal Height Comparison Results.....	23
4.2.2 NJS Tidal Height Comparison Results.....	27
5 SUMMARY .....	33
6 RECOMMENDATIONS .....	35
7 REFERENCES .....	37
APPENDIX—RESULTS FROM LIMITED EVALUATIONS OF PCTides CURRENTS ACCURACY .....	A-1



## LIST OF ILLUSTRATIONS

Figure		Page
1	MLLW Offset for the KTS .....	11
2	NRL LINKS Moorings Locations in the KTS .....	13
3	Locations of the NRL RAGS Moorings Off the U.S. East Coast.....	14
4	Algorithm Sequence.....	15
5	PCTides MLLW Offset Estimates .....	17
6	Bias Errors in PCTides MLLW Offset Estimates.....	18
7	Total Errors in 2-Day PCTides MLLW Offset Estimates .....	21
8	Spring/Neap Cycle Variance in PCTides MLLW Offset Estimates.....	22
9	LINKS Mooring N2 SSH Fluctuations.....	23
10	LINKS Mooring N5 SSH Fluctuations.....	24
11	PCTides Prediction Errors for SSH Highs and Lows in the KTS.....	25
12	Realized PCTides Prediction Errors at the Actual Times of Model-Predicted SSH Highs and Lows in the KTS .....	26
13	RAGS Mooring R1 SSH Fluctuations .....	28
14	RAGS Mooring R6 SSH Fluctuations.....	28
15	PCTides Prediction Errors for SSH Highs and Lows on the NJS.....	29
16	Realized PCTides Prediction Errors at the Actual Times of Model-Predicted SSH Highs and Lows on the NJS.....	30
A-1	LINKS Mooring C1 Tidal Speed.....	A-1
A-2	Realized PCTides Prediction Errors for Tidal Currents at Actual Times of Model-Predicted Peak and Slack Currents.....	A-2
A-3	Tidal Speeds at RAGS Moorings.....	A-4

## LIST OF TABLES

Table		Page
1	Algorithm Descriptions.....	16
2	Error Statistics for PCTides MLLW Offset from 29-Day and 2-Day Runs .....	19
3	Estimated MLLW Offset Errors at LINKS Moorings N2 and N5, Accounting for PCTides Accuracy .....	25
4	SSH Prediction Errors at Times of Model Peaks Compared to MLLW Offset Errors in the KTS .....	26
5	Range Errors and MLLW Offsets on the NJS .....	29
6	SSH Prediction Errors at Times of Model Peaks Compared to the Average MLLW Offset on the NJS .....	30
A-1	Tidal Current Prediction Errors at Times of Model Peak and Slack Tidal Currents for the KTS .....	A-3
A-2	Tidal Current Prediction Errors at Times of Model Peak and Slack Tidal Currents on the NJS.....	A-4

## LIST OF ABBREVIATIONS AND ACRONYMS

AREPS	Advanced Refractive Effects Prediction System
ASW	Antisubmarine warfare
C4ISR	Command, control, communications, computers, intelligence, surveillance, and reconnaissance
CNMOC	Commander, Naval Meteorology and Oceanography Command
DBDB-V	Digital Bathymetric Data Base—variable (resolution)
DII COE	Defense Information Infrastructure Common Operating Environment
DISA	Defense Information Systems Agency
DoD	Department of Defense
GCCS-M	Global Command and Control System—Maritime
GFMPPL	Geophysical Fleet Mission Program Library
IHO	International Hydrographic Office
ISR	Intelligence, surveillance, and reconnaissance
KTS	Korea/Tsushima Strait
LLW	Lower low water
METOC	Meteorology and oceanography
MLLW	Mean lower low water
MLW	Mean low water
MSL	Mean sea level
NITES II	Naval Integrated Tactical Environmental System II
NJS	New Jersey Shelf
NRL	Naval Research Laboratory
NSSM	Navy Standard Surf Model
NUWC	Naval Undersea Warfare Center
OAML	Oceanographic and Atmospheric Master Library
PCTides	Personal Computer Tides Model
SFMPPL	Submarine Fleet Mission Program Library
SRB	Software Review Board
SSH	Sea surface height
TE	Total error
UTC	Universal time (coordinated)
UUV	Unmanned undersea vehicle

# **IMPLEMENTATION OF PCTides IN NITES II: A FOCUS ON MEAN LOWER LOW WATER REFERENCE**

## **1. INTRODUCTION**

This technical document presents the potential for referencing predicted tidal height outputs from the Naval Research Laboratory PCTides model to Mean Lower Low Water (MLLW). Currently, the model's tidal height predictions are referenced to Mean Sea Level (MSL). These predictions cannot always be directly used by warfighters to support tactical decision making.

The errors introduced by assumptions used in changing the baseline reference to MLLW are reviewed using model runs and measured data sets for challenging environments in the western Pacific. The direction and magnitude of the introduced errors are compared to the PCTides model errors that occur with the present design and MSL baseline.

Section 2 provides background information on the Naval Integrated Tactical Environmental System II (NITES II) software program that supports tactical decision making.

Section 3 discusses the methods, test regions, and databases for analysis of PCTides performance and for testing of new algorithms. PCTides model errors were evaluated using NITES II for the Korea Tsushima Strait and the New Jersey Shelf area. A complete algorithm to convert from an MSL to an MLLW reference using information that could be provided by PCTides is presented.

Section 4 evaluates the methods for referencing the tidal height predictions to MLLW. MLLW offsets from MSL are calculated from simulated PCTides output and are compared to offsets more accurately determined from tidal coefficients. Additionally, a limited evaluation of the overall accuracy of the PCTides model is made and the implications for MLLW reference conversion are discussed. A comparison of the results of model runs using the two candidate reference baselines (MSL and MLLW) and a review of the inherent PCTides model errors provide a basis for recommendations on PCTides model design and development.

Section 5 provides a summary of the analyses, and section 6 offers recommendations for model development and a roadmap for improved implementation. The recommendations address the issue of re-baselining tidal predictions to MLLW to better support tactical decision makers without sacrificing model accuracy at scales that impact field operations. These recommendations are intended for review by agencies responsible for directing and executing improvements to oceanographic models used for Fleet tactical operations.

## 2. BACKGROUND

This section presents background information on the NITES II and the PCTides model implemented in NITES II. This information provides the framework for evaluating the analyses and recommendations presented in this document.

### 2.1 NITES II

NITES is the U.S. Navy program of record for integrating meteorology and oceanography (METOC) data into command, control, communications, computers, intelligence, surveillance, and reconnaissance (C4ISR) systems. It is a suite of software applications that have been developed to meet the operational requirements of the Navy and Marine Corps, including the integrated requirement sets defined for joint forces support. Development guidelines are aligned with the Navy integrated warfare architectures of sea dominance, air dominance, power projection, and information superiority. The primary objectives are providing battlespace characterization and situational awareness through access and exchange with distributed METOC data sources, visualization of METOC products, and use of decision aids to analyze the impact of weather and oceanographic conditions on weapons/combat systems. Integral to the design and build process are compliance with DII COE standards and GCCS-M requirements. Periodic deliveries are evaluated by the Defense Information Systems Agency (DISA) to ensure conformity. Individual applications within the NITES suite are products of the software development teams directly supporting the program or are integrated products from other DoD sources. In every case, the integration of applications conforms to a modular architecture, streamlining the update, replacement, and addition of components within the suite.

NITES is the most recent product sponsored by the Oceanographer of the Navy (N7C) to integrate METOC information into warfighting systems and tactical decision making. For nearly four decades, an evolutionary line of software products have increased the ability of the warfighting community to access environmental data and apply it operationally for mission planning, increased situational awareness, and direct use in some warfighting systems. Early deliveries of the Submarine Fleet Mission Program Library (SFMPL), and its shoreside counterpart, the Geophysical Fleet Mission Program Library (GFMPL), allowed for basic evaluation of environmental data, including observations, model outputs, and embedded historical data, to support a suite of missions. The SFMPL developed a set of functions specifically to address the ASW priorities of sonar search effectiveness and own-ship vulnerabilities, in addition to supporting weapon pre-set calculations based on oceanographic data. This fledgling capability received considerable emphasis through the early 1990s, and the sophistication of the applications increased rapidly. Improvements in data access, integration, processing, and display were matched by development of acoustic propagation models and algorithms for characterizing sonar system performance. A host of specialized products supported by the Oceanographer of the Navy bloomed from the SFMPL foundation. CAAM, ASWTDA, SIIP, AESS, SPPFS, and STDA represent some of the products that ultimately borrowed from the early SFMPL development. As these systems were fielded and supported on

ashore and afloat platforms, it became clear that a product line that emphasized open-system architecture concepts and modular implementation could reduce the maintenance costs, improve the capability through multiple vendor development and code sharing, and significantly reduce operator training. Functional subsets of the full suite could be easily distributed from the modular build for specific operational applications, and consistency in results would be maintained to support distributed and joint operations. NITES is identified as the program of record to serve in this role, and other fielded systems will be replaced as scheduled system upgrades occur. Today, nearly 120 builds of NITES have been distributed to operational commands, evenly divided between shore commands and tactical platforms at sea.

NITES continues to evolve as new functions and improvements to existing applications add to the capabilities of this software suite. Integration of joint applications are particularly emphasized, and recent additions to the NITES suite include tri-service (Army, Air Force, Navy and Marine Corps) threshold evaluation tools, Advanced Refractive Effects Prediction System (AREPS) for electro-magnetic sensor performance prediction, and Target Acquisition Weapons Software (TAWS) for electro-optical sensor performance prediction. The advent of the joint Environmental Toolkit provides increased impetus to this movement, and alignment with joint products will be a focus of future NITES builds as programs between the forces become more closely aligned.

### ***2.1.1 NITES II Mission Focus***

The functionality provided by the NITES suite is considerable and would prove overwhelming from an operability perspective if not organized into discrete areas. The organization selected for NITES is task-based, and designated user tasks correlate to specific tactical objectives. Twelve user tasks have been defined to partition and organize NITES functionality for access:

- Data Maintenance
- Environmental Analysis
- Meteorological Visualization
- Electromagnetic Sensor Performance Predictions
- Electro-Optical Sensor Performance Predictions
- Battlegroup Predictions (Passive/Active Sonar Performance)
- Joint Forces Threshold Evaluation Tool (Environmental Impact)
- Coastal Predictions (Tides/Surf)
- Hazard Predictions (N/B/C)
- Search and Rescue
- Briefing Preparation
- Brief Administration Tool.

An individual user task may organize a collection of tiered models and sub-tasks that support complex outputs, such as platform/sensor performance evaluations, or they may perform

lower order functions, such as administrative tasks, environmental data access, data visualization, or analyses of environmental parameters.

### ***2.1.2 Coastal Predictions User Task***

The Coastal Predictions User Task allows the NITES II operator to review sea surface heights, currents, and surf conditions for dynamically selected areas of interest and forecast times. This information is critical to coastal operations in the littoral zone, including many naval special warfare missions, amphibious assault planning, deployment of specialized coastal sensors, UUV ISR and survey missions, and similar warfighting tasks executed in shallow-water areas.

The Coastal Predictions User Task in NITES II provides access to sea surface height and surf conditions by accessing physical models integrated into the modular NITES II software suite. The models used in the Coastal Predictions User Task—and the models, databases, and algorithms in all the NITES II User Tasks—are selected from the library endorsed by the Commander, Naval Meteorology and Oceanography Command (CNMOC) through the Oceanographic and Atmospheric Master Library software review board (OAML SRB) when they are available to meet functional requirements. The PCTides model and the Navy Standard Surf Model (NSSM) have been integrated into NITES II to meet the tide and surf prediction requirements because of their approval status with OAML and their ability to meet the operational requirements levied on this user task through Fleet guidance. These models access the standard OAML databases for input of static data parameters (e.g., bathymetry), and utilize grid-field inputs from meteorological and oceanographic models for dynamic data types (e.g., wind speed/direction). Manual inputs from local observations are also allowed.

## **2.2 TIDES MODELING**

### ***2.2.1 PCTides Model***

The NITES II Coastal Predictions User Task supports both tide and surf forecasts. The focus of this document, however, is specifically on the tide model and its implementation. The tide model selected for initial implementation in NITES II is PCTides version 1.0.

PCTides is a physics-based model developed by the Naval Research Laboratory (NRL) Stennis Space Center to predict sea surface heights/times and currents based on tidal and wind forcing (reference 1). It is a re-locatable model that allows grid-field and point predictions at selected areas/locations that are not limited to International Hydrographic Office (IHO) tidal areas and stations. The ability to include wind forcing and to uniquely define new locations for sea surface height/time and current predictions highlights PCTides as the sole candidate to meet Navy/Marine Corps operational requirements for NITES II. To further reinforce the selection, PCTides is the only predictive tide model presently in the OAML review process, and it is the recommended tidal prediction model in the CNMOC functional area management environmental products review.



PCTides implementation in NITES II addresses the immediate requirements of function and endorsement, but several issues have been identified for discussion and development during the implementation review. These issues are associated with the expanded user group expected with distribution of NITES II to operational commands:

- Fleet operators without professional expertise in tidal prediction would be able to define analysis areas that were inappropriate for model runs because the scale, density/quality of tidal stations, bathymetry data resolution, coastal morphology, or other factors, and limiting controls/guidance had not been developed with the model.
- The model had not been developed to interface with some standard Fleet products for environmental data (e.g., COAMPS wind fields) that would be expected with the operational release in NITES.
- Operability (HIS standards) for Fleet operators at ashore and afloat facilities had not been fully considered.
- The model adopted accepted scientific principles in referencing MSL as the baseline for tidal height predictions, precluding direct reference to navigation charts and some decision/reporting tools for coastal operations.

The NRL Stennis Space Center worked directly with the Naval Undersea Warfare Center (NUWC) Division, Newport, RI, and Science Applications International Corporation to provide guidance on software routines that would help the operator to define appropriate bounding of analysis areas. Additionally, they developed code changes to the model to allow expanded environmental data access and reviewed the implementation to assist in improving operability. This assistance by NRL and continuing Fleet review of the initial implementation by the Naval Atlantic Meteorology and Oceanography Detachment Newport, located at the Naval War College, greatly improved the operational value of PCTides in the Coastal Predictions User Task of NITES II. However, a significant issue remains: the reference baseline for sea surface heights is MSL. While this reference is useful in many applications and has been adopted even for some Fleet software (e.g., MEDAL), the sea surface height predictions cannot be directly applied to charted depths for prediction of depth below keel, drying features, bridge clearances, or bottom navigation. Addressing this issue will be critical for expanded use of the Coastal Predictions User Task.

### ***2.2.2 MSL Versus MLLW***

The tide is defined as the periodic rise and fall of water resulting from the gravitational interactions between the sun, moon, and earth (reference 2). These fluctuations in water level must be measured with respect to a vertical datum that is often referenced to a benchmark on the local shoreline. Movement of water with respect to the chosen datum is not only caused by tides, but can have contributions from waves, wind, ocean currents and eddies, water density changes, fluctuations in air pressure, seiches, and relative sea level change (reference 3). In sea surface height measurements, some of these non-tidal effects can be difficult to separate from pure tidal forced changes. However, over long time periods, most of these phenomena average to no



effect, as they are not periodic (as tidal fluctuations are). The combinations of different tidal effects cause slow periodic trends to modulate the daily and/or twice-daily character of tidal fluctuations. The longest period trend that significantly modulates the tides is the 18.6-year period regression of the moon's nodes (reference 3). Because of this, averaging for computation of tidal datums is done using a 19-year period (currently 1960-1978) referred to as the "National Tidal Datum Epoch" (reference 2). The following sections describe two tidal datums (MSL and MLLW) and how they relate to PCTides.

**2.2.2.1 MSL.** MSL is defined as the arithmetic mean of hourly heights observed over the National Tidal Datum Epoch (reference 2). Only sea level forcing functions that have significant means over 19 years can influence MSL. Therefore, MSL is practically independent of all but permanent ocean currents and relative sea level change. In particular, over a 19-year period, tidal fluctuations should have near zero means and, therefore, MSL is independent of the tide. The spatial variations of other tidal datums are dependent on the spatial variations of the character of the tides.

MSL closely approximates the geoid (equipotential gravity surface) and, following this approximation, sea surface height departures from MSL will generate ocean currents. Therefore, it is convenient for numerical models to use a coordinate system referenced to MSL, such that a state of rest in the model system corresponds to no initial currents and zero sea surface height at MSL. PCTides and almost all numerical models use this convention. The vertical datum for DBDB-V, the bathymetry used in PCTides, is also MSL (reference 4).

**2.2.2.2 MLLW.** MLLW is defined as the average over the National Tidal Datum Epoch of the Lower Low Water (LLW)—the lowest height of the day induced by the tides—of each day (reference 2). This datum is explicitly defined such that it is dependent on the character of the tides at each location. Therefore, a spatial function that depends only on tides can be added to MLLW (defined by tides) to convert it to MSL (practically independent of tides).

The depth of the water on nautical charts is referenced to MLLW for U.S. charts (see reference 3). This is a conservative reference that ensures that the water depth is above the chart depth at most times. For a mariner to accurately reference predicted tidal height fluctuations to chart depths, both the predicted height from MSL (from available prediction systems such as PCTides) and the local MLLW to MSL offset must be known.

### 3. METHODOLOGY

This section presents information on the methods used in this study to conduct research on changing the reference level of PCTides from MSL to MLLW. In principle, the conversion of an MSL to an MLLW reference can be accomplished by determining a spatially dependent offset from tidal sea-surface height (SSH) fluctuations. Section 3.1 presents such a method appropriate for the IHO tidal database or other coefficient databases. Section 3.2 describes a coefficient database and two measurement datasets used in this study for the analysis of proposed algorithms and PCTides output. The PCTides model does not represent tides in coefficient form or provide long time series of tidal fluctuations. Therefore, an alternate (empirical) method is presented in section 3.3 to derive MLLW offsets from PCTides outputs.

#### 3.1 CALCULATING MLLW OFFSETS FROM TIDAL COEFFICIENTS

Although calculating MSL to MLLW offsets from tidal coefficients is straightforward in theory, no standard tools exist to support this. Therefore, a MLLW offset calculator that accepts tidal coefficients for inputs was developed for this evaluation and possible future application to PCTides upgrades. The calculator operates by reconstructing 19-year time series and then applying the formal definition of MLLW (section 2.2.2.2) to the reconstruction.

It is important to the accuracy of the calculator that nodal cycles be included in the 19-year time series reconstructions. The Foreman (reference 5) tidal analysis software adapted to MATLAB by Pawlowicz, Beardsley, and Lentz (reference 6) was used for time series reconstruction, but their codes made a single nodal adjustment at the center time point because they assumed that the requested time series duration would be small compared to the nodal period. This code was modified for the offset calculator to make a nodal adjustment approximately every 10 days so that reconstructed 19-year time series would include a nodal cycle. Including the nodal cycle in the reconstruction significantly slows down the algorithm.\*

The MLLW offset calculator software developed for this study takes tidal coefficients and the latitude of a particular site as inputs, calls the modified Foreman (reference 5) package to reconstruct a 19-year time series<sup>†</sup> of SSH, and calculates the average of the depth below MSL of the LLW. This final calculation gives the output value of the software; this is subtracted from time series referenced to MSL to convert to a MLLW reference. The software could be easily modified to allow the selection of alternative references to remain consistent with operational/navigational charts (e.g., MLW).

---

\*Algorithm slowed from 2.3 to 11.5 seconds per reconstruction on a 3.1-GHz Pentium 4 computer.

<sup>†</sup>Currently set to be the 19 years before the present date, but should be adjusted in future implementations to be the National Tidal Datum Epoch for consistency.

## 3.2 TEST REGIONS AND DATABASES

This study required specific areas to test MSL-to-MLLW conversion methods and to analyze these methods in conjunction with PCTides output. Two regions of differing tidal character with readily available data were selected for testing: the Korea/Tsushima Strait (KTS) and the outer New Jersey Shelf (NJS).

The tides of the KTS exhibit a high degree of spatial variability. The tidal range is high in the southern and western end of the strait, but very low in the northern end. The character of the tides also undergoes a significant spatial change in the strait since the relative importance of individual tidal constituents shifts as the tide propagates through the strait (reference 7)). These facts make the KTS a good location for testing MLLW offset methods because the algorithm will be tested to reproduce the strong spatial gradient in MLLW offset and over different tidal regimes. Therefore, this region was chosen as the main location for testing and PCTides analysis.

In contrast, the tides on the outer NJS change gradually, and the relative importance of individual tidal constituents does not shift greatly. This region was selected as a contrast to the KTS for PCTides analysis. The KTS is expected to be a relatively challenging region for tidal prediction, while the NJS is expected to pose an easier challenge for tidal prediction.

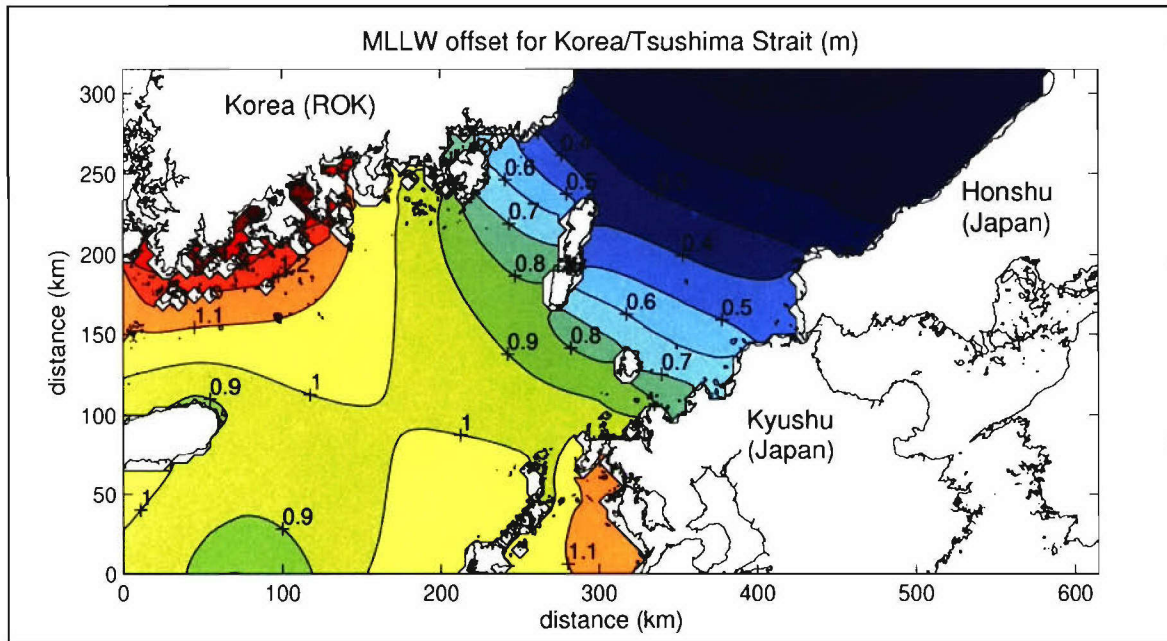
### 3.2.1 *Developing an Algorithm Test Database and Simulating Algorithm Implementation*

An existing tidal coefficient database was used with the offset calculator described in section 3.1 to build a grid of MLLW offsets for comparison with empirically calculated MLLW offsets (section 3.3). The NRL KTS tidal database is a product from the High-Resolution Coastal Currents project funded by the Space and Naval Warfare Systems Command's (PMW 150) Operational Effects Program. This database provides a 5x5-km grid of eight tidal constituents determined by a barotropic model that assimilated\* tidal data from 73 stations scattered throughout the KTS. Rms errors in model tidal coefficients are less than 3 cm over most of the domain and less than 0.5 cm in portions of the Strait (reference 7).

The coefficients from the KTS database were used as inputs to the MLLW offset calculator developed in this study to produce a spatial grid of MLLW offsets for the KTS. Figure 1 presents these offsets, i.e., the difference between MSL and MLLW in meters. The location of the origin in figure 1 is (32.59533° N, 126.2005° E).

---

\*Strong-constraint variational data assimilation using an adjoint model.



**Note:** Contoured offset values (meters) to add to time-series referenced to MSL to convert to an MLLW reference for the KTS. The origin is 32.59533° N, 126.2005° E. The KTS has a complicated offset field with a wide range of offset values.

**Figure 1. MLLW Offset for the KTS**

The available NITES II implementation of PCTides was not built to provide the appropriate outputs for testing algorithms, e.g., IHO data and information are stored internally, the closest IHO stations are not reported externally, the external reporting style of SSH peaks and lows is difficult to use, etc. Therefore, it was more efficient to test proposed algorithms using simulated PCTides output rather than actual PCTides output. The NRL KTS tidal database was also used for this purpose. A 29-day duration time series for the entire spatial grid was constructed, and tidal ranges and LLW values were calculated. The 29-day period (nearly synodic) was chosen to minimize the effect of strong tidal range variance over the spring/neap cycle. Some tests were also performed to study the spring/neap induced error in the offset results by using more typical 1- to 8-day time series durations. Actual IHO station positions were used; but, for consistency of comparison with MLLW offsets calculated using coefficients, tidal range and LLW values for IHO stations were also constructed from the KTS tidal database. Only IHO stations actually located in the strait with measurement durations exceeding 1 year were considered, and only the eight tidal constituents from the KTS tidal database were used.

### 3.2.2 PCTides Runs and Measurement Datasets Used for Tidal Prediction Comparisons

PCTides provides predictions for tidal height and current fluctuations, and these predictions will naturally have errors associated with them. These errors will impact empirical methods to derive MLLW offsets using PCTides outputs. Therefore, to help understand introduced error for the MLLW offset that would occur from non-perfect PCTides inputs, brief analyses of PCTides output and comparisons to measured data were performed for the two test regions.



For both comparisons, PCTides domains were set up and run using the Coastal Predictions User Task in the current build of NITES II. The results of these runs were compared to directly measured tidal data from moorings deployed in the region of interest. To extract only tidal information and to project measurements forward to specific time periods, tidal coefficients were calculated from the measurements. Then, for selected 2-day periods, new (tide only) time series were generated using Foreman (reference 5) tidal analysis software adapted to MATLAB by Pawlowicz, Beardsley, and Lentz (reference 6). The time series synthesized by measurements were then compared to the tabular output of maximum/minimum heights from the TIDES function of the Coastal Predictions User Task. This was done for the KTS using the NRL LINKS dataset (reference 8) and for the NJS region using the NRL RAGS dataset (reference 9).

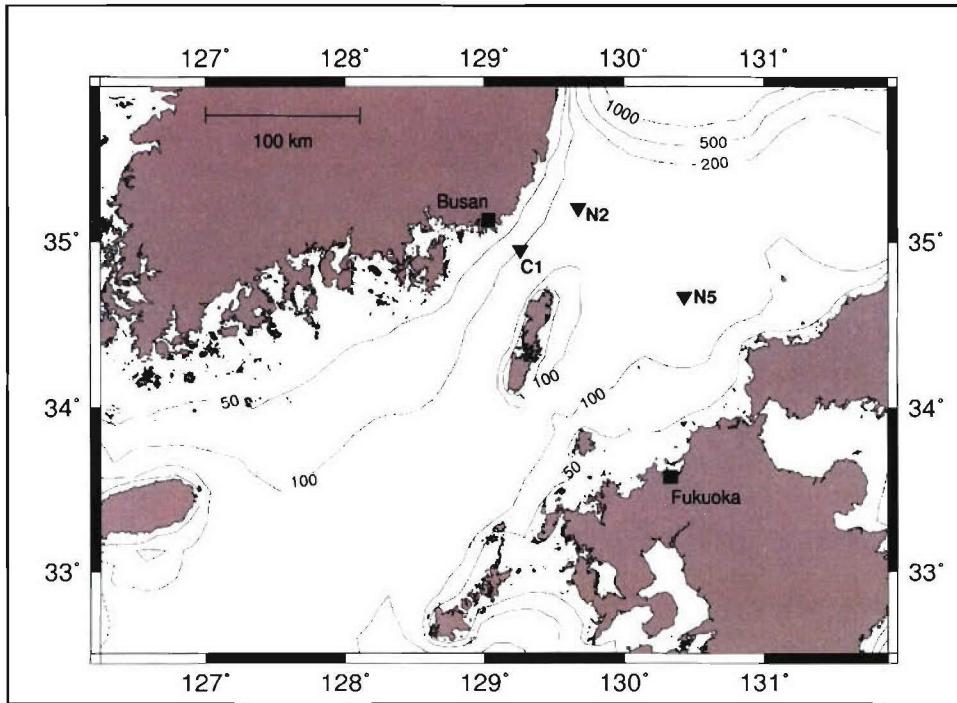
**3.2.2.1 Setup for NITES II PCTides, KTS Comparisons.** Figure 2 shows the locations of selected NRL LINKS moorings deployed during the period May 1999 through March 2000 in the KTS (reference 10). From a large array of data sites, three high-quality sites that are relatively close together with differing characteristics were selected for PCTides prediction and comparison. Selected site N2 has larger tidal currents but smaller tidal height fluctuations than selected site N5. Tidal heights were not measured at selected site C1;\* however, this site has the largest tidal currents and should pose the greatest challenge for current prediction because it is located in the channel between Korea and Tsushima Island. Tidal coefficients (see reference 2) used for time-series synthesis are  $O_1$ ,  $P_1$ ,  $K_1$ ,  $\mu_2$ ,  $N_2$ ,  $M_2$ ,  $S_2$ , and  $K_2$ . (See reference 7 for measurement details.)

The main domain (big grid) for the KTS was selected as the 340-km by 658-km box extending from (36°17'2"N, 125°53'58"E) to (33°13'42"N, 132°58'55"E). The maximum allowable grid resolution was selected for this domain, which divided the 340-km east/west sides into 150 grid points, thus setting the domain grid size to 2.3 km everywhere. The run of the tides function was done without winds, and output was requested at the locations of moorings C1, N2, and N5 (as discussed above). The run was executed for 2 days starting on 11 November 2004 at 00:00 UTC. This period is a time between the spring and neap times for tidal currents and should be representative of typical tide conditions. PCTides simulates the  $Q_1$ ,  $O_1$ ,  $P_1$ ,  $K_1$ ,  $2N_2$ ,  $N_2$ ,  $M_2$ ,  $S_2$ , and  $K_2$  tides. The differences in tidal constituents that are considered between the measurements and model should not cause large disagreements because for the KTS,  $Q_1$ ,  $2N_2$ , and  $\mu_2$  are all much smaller than the other seven matching constituents.

---

\*Tidal current comparison was performed, but, since the accuracy of PCTides current prediction does not impact MLLW offset calculation, this comparison is included in the appendix.

Two other PCTides domains were selected to test the sensitivity of model results to domain size and resolution. The second domain (small grid) is 127 km by 239 km extending from (35°42'32"N, 128°23'11"E) to (34°34'8"N, 130°59'45"E). Again, the maximum allowable grid resolution was selected to produce a 0.8-km grid spacing. The third domain (nested grid) was an 84-km by 100-km nested-grid\* extended from (35°17'13"N, 128°22'40"E) to (34°31'44"N, 129°28'55"E) and embedded in the big grid domain; this domain was used only for current evaluation (see the appendix).



**Note:** NRL LINKS moorings are shown as triangles and bathymetric contours for the 50-, 100-, 200-, 500-, and 1000-m isobaths are drawn as thin lines (reference 10). Tsushima Island is the large pair of islands in the center of the map. Kyushu is the main Japanese island in the southeast portion of the map and Honshu is the main Japanese island north of Kyushu.

**Figure 2. NRL LINKS Moorings Locations in the KTS**

**3.2.2.2 Setup for NITES II PCTides, NJS Region Comparisons.** From late November 2003 to early February 2004, six moorings were deployed across the NJS region as part of the NRL RAGS project (reference 9). Tidal characteristics change very gradually in this region and, therefore, only the inshore mooring (R1) and the offshore mooring (R6) were used for comparisons to PCTides output. The mooring locations are shown in figure 3. Tidal coefficients used for time-series synthesis are  $Q_1$ ,  $O_1$ ,  $K_1$ ,  $J_1$ ,  $\mu_2$ ,  $N_2$ ,  $M_2$ ,  $L_2$ , and  $S_2$ . The strongest tides are  $M_2$ ,  $N_2$ ,  $K_1$ ,  $S_2$ , and  $O_1$ , but the mooring deployments were too short to accurately analyze for  $P_1$ ,  $2N_2$ , and  $K_2$ .

\*The nest used 0.8-km grid spacing (the system crashed for attempts at higher resolution).

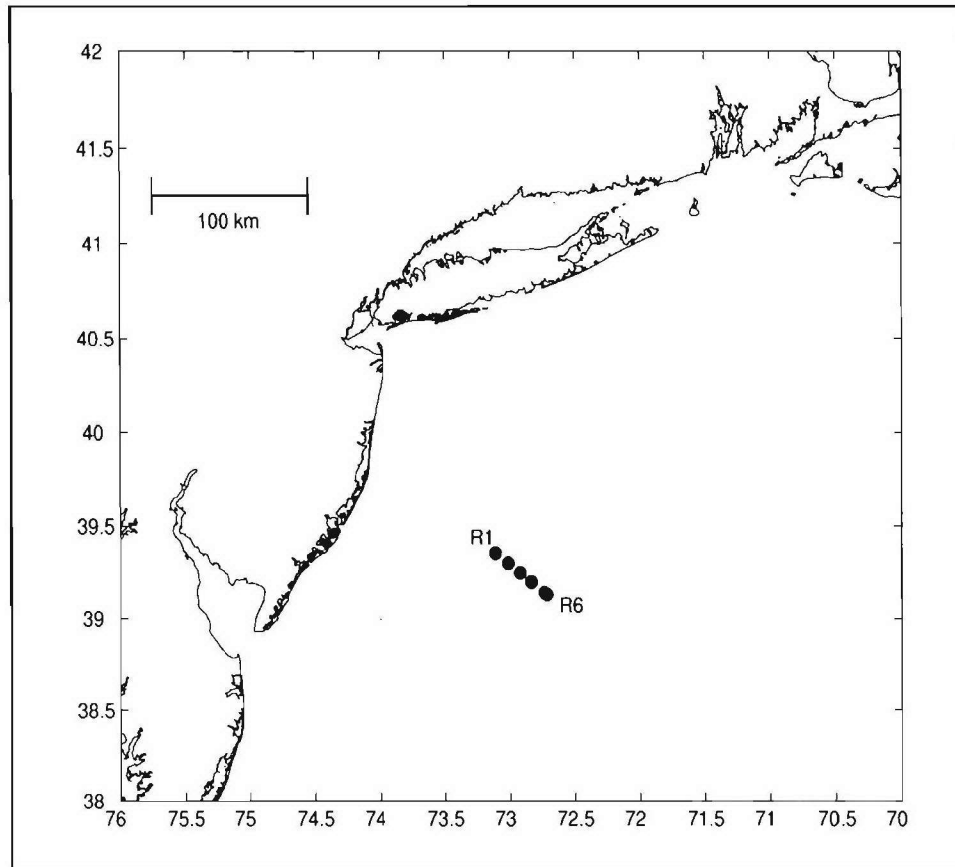


**Figure 3. Locations of the NRL RAGS Moorings (Circles) Off the U.S. East Coast**

Only one PCTides domain was used for the NJS region. The domain was selected as the 333-km by 386-km box extending from (41°00'00"N, 75°30'00"E) to (38°00'00"N, 71°00'00"E). The maximum allowable grid resolution was selected for this domain, which divided the 333-km east/west sides into 150 grid points, thus setting the domain grid size to 2.2 km everywhere. The run of the tides function was done without winds, and output was requested at the locations of moorings R1 and R6, as discussed in the previous paragraph. The run was done for 2 days starting on 25 May 2005 at 00:00 UTC. This period is a time between the spring and neap times for tidal currents and should be representative of typical tide conditions. The exclusion of  $P_1$  and  $K_2$  from the measurement analysis may impact the comparison as PCTides includes these constituents and their equilibrium tidal potential amplitudes are large (the fifth and eighth largest equilibrium tidal potential, respectively). The lack of  $J_1$ ,  $\mu_2$ , and  $L_2$  in PCTides predictions will contribute to differences as these amplitudes are small but significant in the RAGS array; in particular,  $\mu_2$  amplitudes are almost 3 cm at both R1 and R6.



### 3.3 DEVELOPING AN ALGORITHM TO CALCULATE PCTides MLLW OFFSETS

PCTides does not output tidal coefficients, and the section 3.1 MLLW offset calculator cannot be used for conversion of MSL to MLLW in this model. An alternative method for calculating the offset is required.

In typical NITES II usages, PCTides provides 1- to 7-day duration time series predictions of SSH fluctuations throughout the user-selected domain at user-selected stations. IHO tidal station data are used by PCTides for data assimilation and; therefore, the model has access to this database. Unless major changes are implemented in PCTides, a MLLW offset for PCTides must be calculated from these limited data resources. All information on *spatial variability* away from the coasts must come from short duration time series. All information about the *phase of the tidal fluctuations* with respect to monthly and longer cycles must come from the IHO stations.

Several algorithms for calculating MLLW offsets were investigated, each using the ratios between sites in tidal range or LLW height averaged over short time periods to deduce the spatial change in MLLW offset. Such algorithms should perform well for most parts of the ocean because the spatial change in MLLW offset is relatively gradual. The algorithm in figure 4 produced the lowest error for 2-day time series, which are expected to be typical of PCTides usage (see section 4).

**Step**

1. For a given spatial point, the closest long-duration IHO station reporting all primary tidal coefficients is identified.
2. The MLLW offset is calculated for this station using the MLLW offset calculator for tidal coefficients (section 3.1).
3. The daily tidal ranges for the period of the PCTides run are calculated at this station from PCTides time series outputs.
4. The daily tidal ranges for the given spatial point are calculated from PCTides time series outputs.
5. The estimated MLLW offset is given by

$$MLLW_X = MLLW_{IHO} \cdot \frac{\langle range_X \rangle}{\langle range_{IHO} \rangle}$$

with MLLW as the respective offsets, range as the respective daily tidal ranges, and the over-bars denoting averaging of the daily ranges.

**Figure 4. Algorithm Sequence**

Three other variations on this algorithm were investigated. They differed from the above sequence by using LLW in place of tidal range for steps 3, 4, and 5, and/or using the average of the daily ratios instead of the ratio of the average daily ranges/LLW for step 5. Table 1 details the differences between the algorithms. The algorithm that is boxed in figure 4 is algorithm 4 and is the one referred to throughout this document unless another algorithm is explicitly mentioned.

The use of inverse range-weighting algorithms to consider multiple IHO reference stations was not included in this study. Development of algorithms to filter candidate stations for applicability, in addition to range, will promote use of a range-weighting approach in future studies to eliminate discontinuities in basin error predictions.

*Table 1. Algorithm Descriptions*

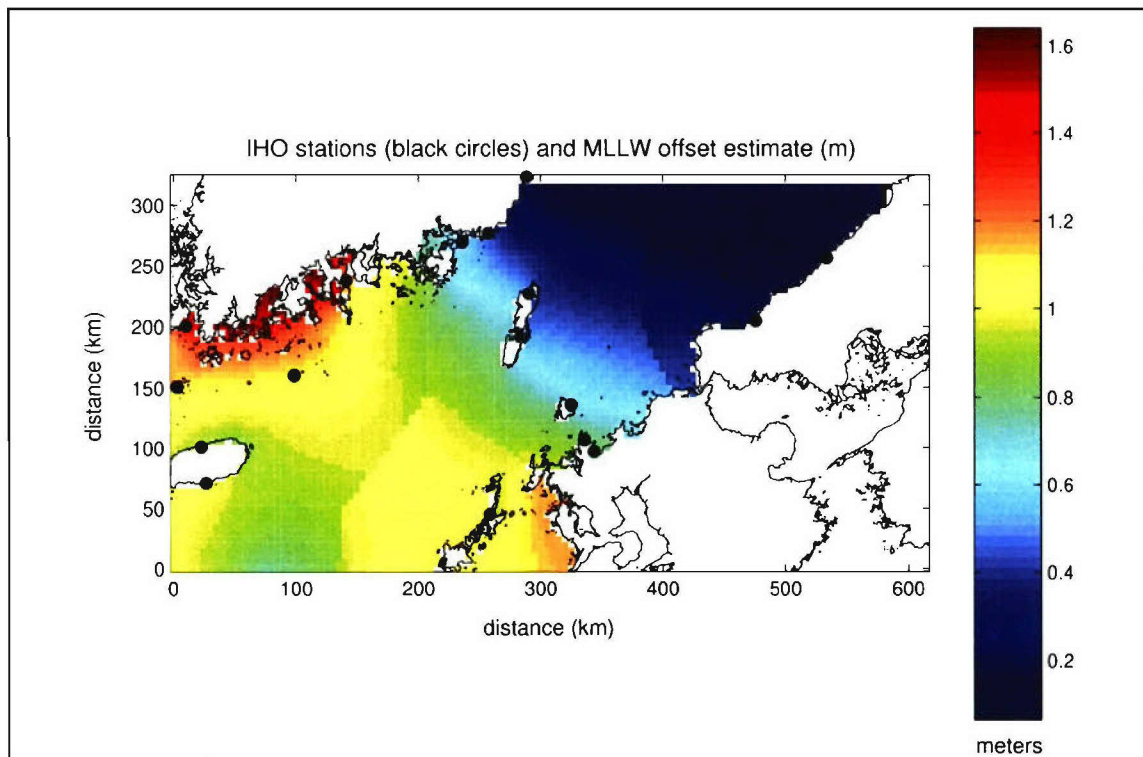
<b>Algorithm</b>	<b>Time-Series Parameter</b>	<b>Average Method</b>
1	LLW	Average of the Ratios
2	LLW	Ratio of the Averages
3	Tidal Range	Average of the Ratios
4	Tidal Range	Ratio of the Averages

## 4. RESULTS AND ANALYSIS

This section presents the results and analysis of this study. Section 4.1 analyzes the accuracy of the conversion algorithm and discusses practical implementation issues. Section 4.2 provides a limited evaluation of overall PCTides model accuracy for the KTS and NJS, and relates PCTides accuracy to the MSL/MLLW reference conversion.

### 4.1 EFFECTIVENESS OF THE PCTides MLLW OFFSET ALGORITHM

The accuracy of MLLW offsets calculated using the algorithm of section 3.3 for the KTS can be evaluated by comparing these offsets to those calculated more exactly using the tidal coefficient database (figure 1). Figure 5 shows the results of applying the algorithm to simulated PCTides output. These results are compared to those shown in figure 1 and discussed in section 4.1.1. The algorithm must also be evaluated on practical implementation issues and compatibility with the present PCTides (section 4.1.2).

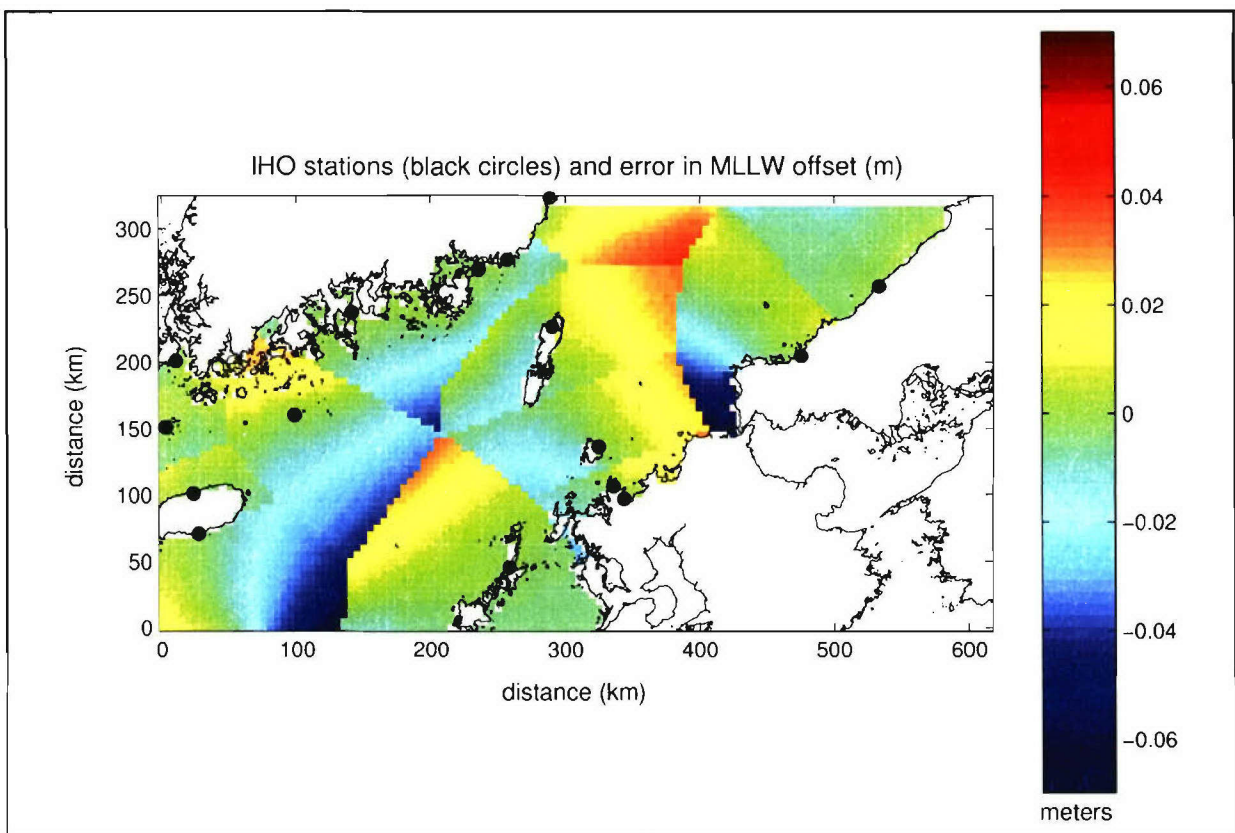


**Note:** Results from applying the algorithm from section 3.3 (figure 4) to the simulated 29-day PCTides outputs. Colors indicate estimated values in meters to add to MSL referenced time-series to convert to MLLW referenced time-series. The black circles are the IHO station locations used in the algorithm.

*Figure 5. PCTides MLLW Offset Estimates*

#### 4.1.1 Simulated PCTides MLLW Offsets Compared with Coefficient Calculated Offsets

Figure 6 shows the difference between MLLW offsets calculated from the KTS coefficient database and the offsets estimated using the algorithm from section 3.3 with 29-day duration simulated PCTides outputs (starting on 13 April 2005). Because the KTS database is considered “truth” for the purposes of evaluating the algorithm, and the simulated IHO coefficients were obtained by interpolation/extrapolation from the KTS database, the zero-error contour must pass through the IHO station locations. This is in agreement with the definition of the algorithm—at IHO station locations the ratio of ranges becomes one, and the estimated MLLW offset becomes the real IHO MLLW offset. Away from IHO station locations, the error can be negative or positive as the ratio of ranges can either over-correct or under-correct for spatial changes in MLLW offset. The error is discontinuous along curves made up of points that are equidistant from two IHO stations. This effect could be smoothed away if the algorithm was improved such that  $MLLW_{IHO}$  was defined through an interpolation scheme using several stations instead of MLLW at the closest station.



**Note:** Error from using the algorithm in section 3.3 (figure 4) to estimate MLLW offsets. The colors indicate the difference in meters of the values from the algorithm applied to the simulated 29-day PCTides and the values calculated from tidal coefficients. Positive differences indicate that the algorithm overestimates the offset and negative differences indicate that it underestimates the offset. The black circles are the IHO station locations used in the algorithm (zero error points)

**Figure 6. Bias Errors in PCTides MLLW Offset Estimates**



For this test, the maximum overestimate (estimated MLLW level lower than the true MLLW level) is 0.04 m and the maximum underestimate is 0.07 m. The percentage error from use of the estimation algorithm is less than 10%, except for the north-central most section of the KTS, where the MLLW offset is small.\* A few isolated places in the main KTS have percentage errors between 5% and 10%. However, the bulk of the KTS has percentage errors less than 5%. Table 2 provides detailed statistics for this 29-day test.

**Table 2. Error Statistics for PCTides MLLW Offset from 29-Day and 2-Day Runs**

	<b>Avg Error (cm)</b>	<b>Max Over-Estimate (cm)</b>	<b>Max Under-Estimate (cm)</b>	<b>Avg Std Err. (cm)</b>	<b>Avg. Total Err. (cm)</b>	<b># &gt;10% (Grid Pts)</b>	<b>10%&gt;#&gt;5% (Grid Pts)</b>	<b>#&lt;5% (Grid Pts)</b>
<b>29-Day Run</b>	1.3	4.1	7.0	---	1.3	309 (7%)	366 (8%)	3718 (85%)
<b>2-Day Runs</b>	1.2	22.1	28.0	2.2	2.7	6964 (11%)	9715 (15%)	49216 (75%)

The MLLW offset estimation algorithm is able to produce variability away from the IHO stations that is in qualitative agreement with the true MLLW offset field (figures 1 and 5). The MLLW offset algorithm matches the low around map coordinate (100, 0), which is about a 100-km distance from the closest station. The eastern part of the low in the north (450, 310) is accurately captured by the ratio of ranges from a 100-km distance station on Honshu, Japan. The regions surrounding Tsushima (the large islands near the center of the KTS) of drastic MLLW offset change have relatively low error (figure 6), even though the estimation of the 0.6-m change is anchored by only four IHO stations. The ability to reproduce these features depends on the ability to accurately estimate the ratio of ranges from the IHO stations to the open ocean. The accuracy of the ratio of ranges for PCTides is analyzed in section 4.2.

#### **4.1.2 Implementation of the MLLW Offset Algorithm in PCTides**

Implementing the algorithm from section 3.3 (figure 4) into PCTides requires identification of applicable IHO tidal stations from the general IHO database and the use of tidal coefficients from the IHO stations thus identified. Wind-generated surge predictions will interfere with calculating accurate tidal ranges from PCTides output. Also, to achieve the figure 6 level of accuracy, 29-day time series from all positions of interest are required.

---

\*At (400, 305) the MLLW offset magnitude is 0.08 and the percentage error is maximum at 43%.

**4.1.2.1 IHO Station Selection.** There is a wide range of accuracy in the IHO station data (reference 7). Some data are derived from a month or less of measurements and are relatively inaccurate or missing key tidal constituents. A key contributor to the success of the section 3.3 algorithm was limiting the IHO coefficients to those stations with at least 1-year duration and at least eight tidal coefficients. Areas of low error (figure 6) extend quite far from these good IHO stations, and it is likely better to continue to use these stations at a distance rather than switch to closer, but less accurate, stations. The duration and number of coefficients should be included as parameters in the internal IHO files. The addition of a station selection routine for the beginning of the run will be needed for PCTides. The routine would identify and select a small subset of the best tidal stations in the domain for use in the MLLW algorithm.

For the algorithm of section 3.3, some IHO stations that passed the duration and number of coefficients tests were not used because they were not located in the KTS. An intelligent spatial sorter might need to be added to PCTides to accomplish such exclusion. Without this, significant error can be introduced if the shortest path between the grid point of interest and the nearest selected IHO station crosses land or another blocking feature. In such cases, the IHO station and the tides at the point of interest could be completely unrelated and the algorithm would provide erroneous results. For example, IHO stations in the Inland Sea (470, 130) should not be used to derive MLLW offsets (figure 5) for tidal predictions along the southwest coast of Honshu, Japan (420, 170) because the tides in the Inland Sea and KTS differ drastically.

**4.1.2.2 Wind Forcing.** A user of PCTides has the option to add wind data to the model run and calculate the combined effect of wind-generated surge and tides. When this is done, the range values from the model required for the algorithm described in section 3.3 would no longer be just tidal ranges. The wind contribution could dramatically affect the ratio of mean ranges and introduce large errors in the MLLW offset calculation. To avoid this problem, the model should be run twice, first without using the winds to calculate the MLLW offset, then using the winds as the user requested. Model run-time will approximately double.\*

**4.1.2.3 Time Series Duration.** The 29-day time series were used for section 4.1.1 to avoid bias from the spring/neap tidal cycle. However, 1- to 8-day duration time series are more typical user selections for PCTides. To explore the effect of using 1- to 8-day time series on the estimation of the MLLW offset, a series of MLLW estimates was made with shorter time series started at various times in the spring/neap cycle.

A 2-day duration run was chosen as a representative PCTides run for the purposes of evaluating MLLW offset algorithms. For the short time series produced by such a run, two errors must be considered: the bias of the algorithm independent of the spring/neap cycle<sup>†</sup> and the variation from choosing a particular 2-day period inside the 29-day spring/neap cycle.

---

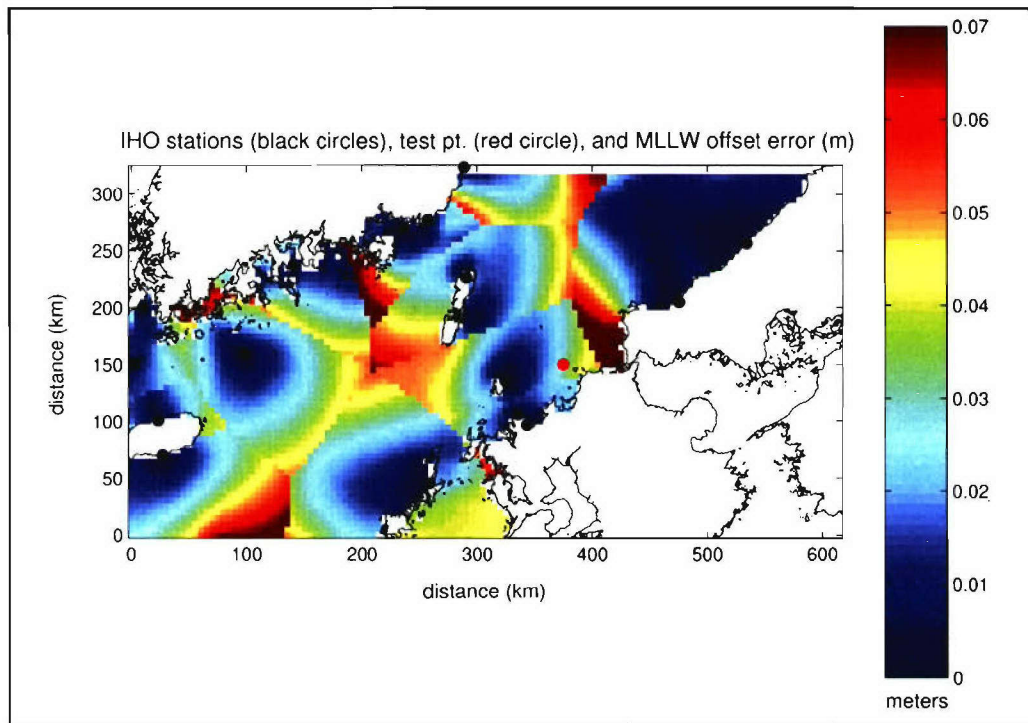
\*Model run times vary. A PCTides run for the NJS domain on a 2.8-GHz Pentium 4 computer took 4 minutes, 6 seconds.

<sup>†</sup>Approximately equal to the error from the 29-day-duration simulations (figure 6).

For algorithm comparisons, an MLLW offset estimate was calculated for 15 different 2-day periods at every point in the KTS using the four algorithms (table 1). Thus,

$$TE = \sqrt{\left(\overline{MLLW_X} - MLLW_C\right)^2 + \sigma_{MLLW_X}^2} .$$

The total error (TE) for each KTS point is with  $MLLW_X$  as the 15 MLLW estimates from the algorithm and  $MLLW_C$  as the MLLW value calculated from the coefficient database. The overbar and sigma represent the mean and standard deviation of the 15 values, respectively. Algorithm 4 presented in section 3.3 had on average the lowest TE of the four algorithms. If 2-day time series are used for estimating MLLW instead of 29-day time series, the expected error magnitude would be these TE values (figure 7) instead of the magnitude of the error values from figure 6. Detailed error statistics for the set of 2-day runs are provided in table 2.

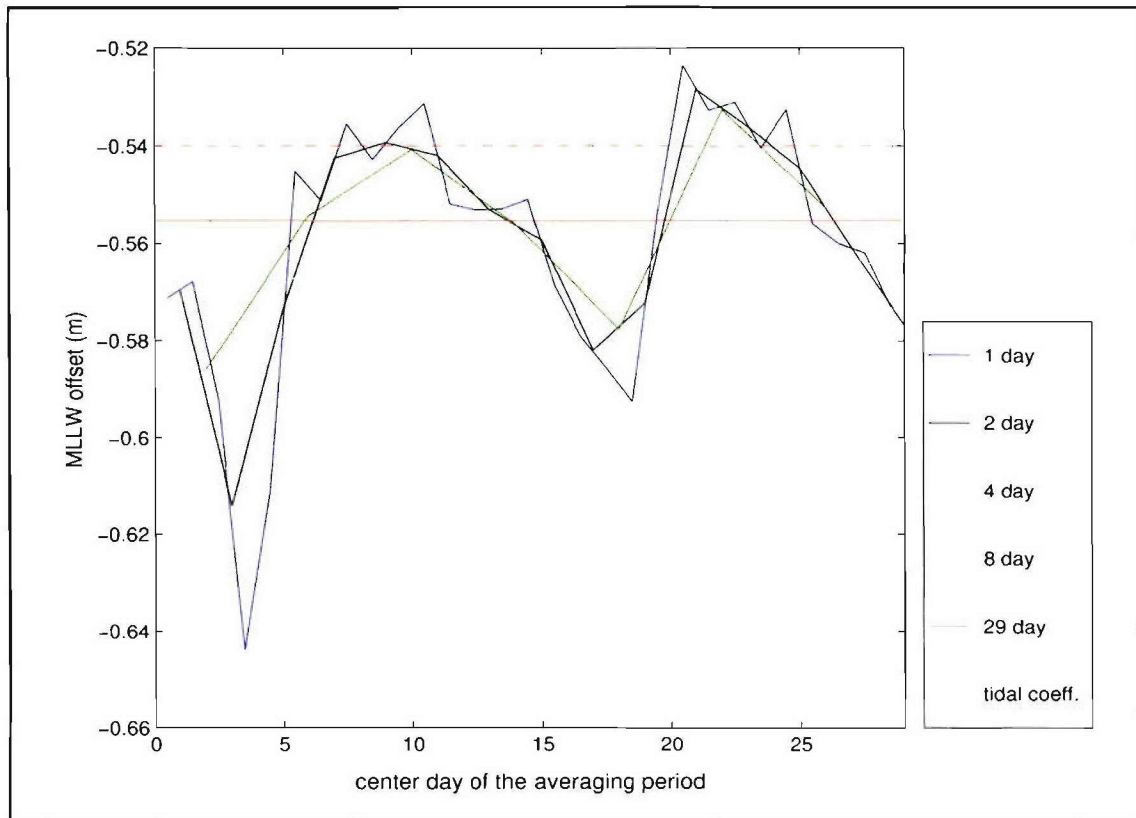


**Note:** Error from using the algorithm in section 3.3 to estimate MLLW offsets with only short time-series inputs. The colors indicate the expected error of the algorithm applied to the 2-day PCTides inputs as compared to values calculated from tidal coefficients. These errors include both the biases and the standard deviations over the spring/neap cycle. The black circles are the IHO station locations used in the algorithm (zero error points). The red circle indicates a spatial point with typical error where tests with various time-series durations were performed (see figure 8).

**Figure 7. Total Errors in 2-Day PCTides MLLW Offset Estimates**



To evaluate the effect of time series durations other than 2 days or 29 days, a point with a typical TE value was selected (red circle in figure 7) and MLLW values were estimated from different 1-, 2-, 4-, 8-, and 29-day time series. As the averaging period increases, the variability over the spring/neap cycle decreases (figure 8).



**Note:** Results from using the algorithm in section 3.3 with simulated PCTides time series spaced equally through the spring/neap cycle compared to a value calculated from tidal coefficients. These estimates were all made for the same spatial point (375,150) where the 2-day error (see figure 7) was closest to the average for the KTS. The key shows the duration of each time-series used to produce the MLLW offset estimates (points on the various curves).

**Figure 8. Spring/Neap Cycle Variance in PCTides MLLW Offset Estimates**

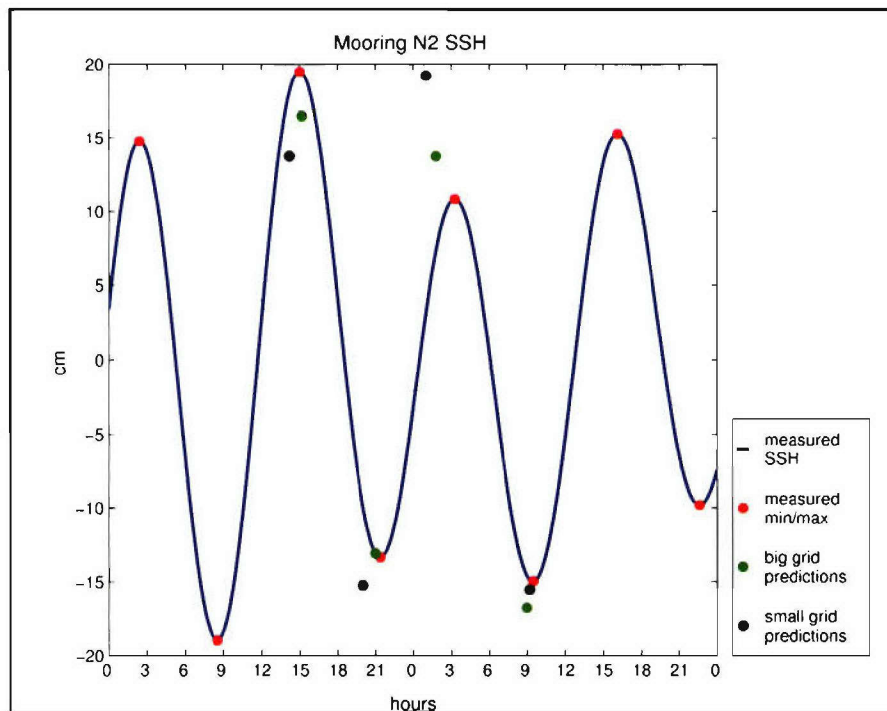
If access to longer PCTides time series is guaranteed—thus reducing or eliminating the relative importance of the standard deviation term in TE—a different algorithm should be considered. Algorithm 2 of section 3.3 produces MLLW estimates with the lowest average bias. This algorithm uses LLW (as is used in the exact definition of MLLW) and was more accurate than the other algorithms for 29-day time series. However, as seen in figure 8, the standard deviation term can be the highest term in the TE formula. Algorithm 4 has the lowest average TE because it has the lowest average standard deviation term for a 2-day time series. Using the range instead of LLW approximately doubles the number of input points to the formula and, thus, is better able to reduce the standard deviation error term. Thus, algorithm 4 is the most accurate for 2-day time series.

## 4.2 RESULTS FROM LIMITED EVALUATIONS OF PCTides SSH ACCURACY

NITES II PCTides predictions and tidal information from measurements were compared to assess the general accuracy of PCTides predictions and the impact PCTides errors would have on the MSL-to-MLLW reference conversion. Results of the comparisons from the KTS (section 4.2.1) could be compared to the estimated accuracy of the MLLW offset that would be calculated from the implementation of the algorithm in section 3.3. Results from the comparison on the NJS (section 4.2.2) provide further data for analysis of PCTides accuracy and comparisons between error levels and MLLW offset values.

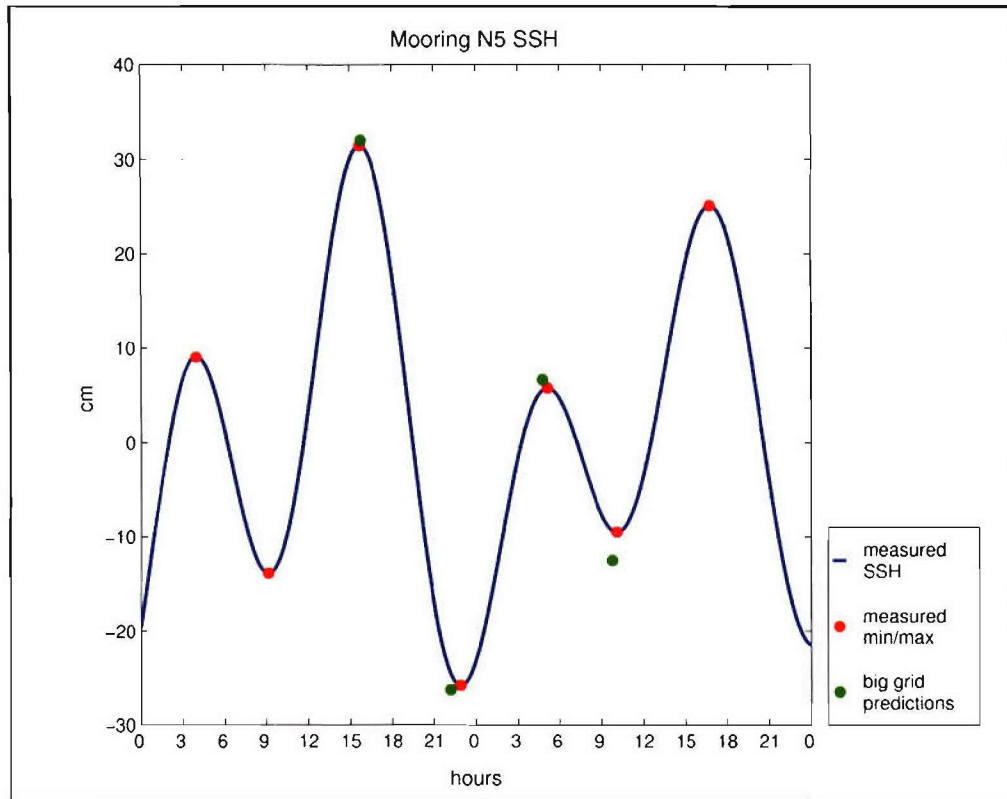
### 4.2.1 KTS Tidal Height Comparison Results

Figures 9 and 10 show the tidal heights synthesized from measurements for the KTS compared to the tabular output from the big grid and small grid NITES II PCTides runs described in section 3.2.2.1. Comparisons were only done for the central highs and lows to avoid any possibility of start-up or end-time model problems. The differences between the model and measurements are presented in figures 11 and 12, respectively, and tables 3 and 4.



**Note:** SSH fluctuations (blue line) projected from measured tidal coefficients at NRL LINKS mooring N2 (see figure 2). The green dots (big grid) and the black dots (small grid) are the predicted maximum and minimum points from the tabular output of PCTides simulations run inside NITES II.

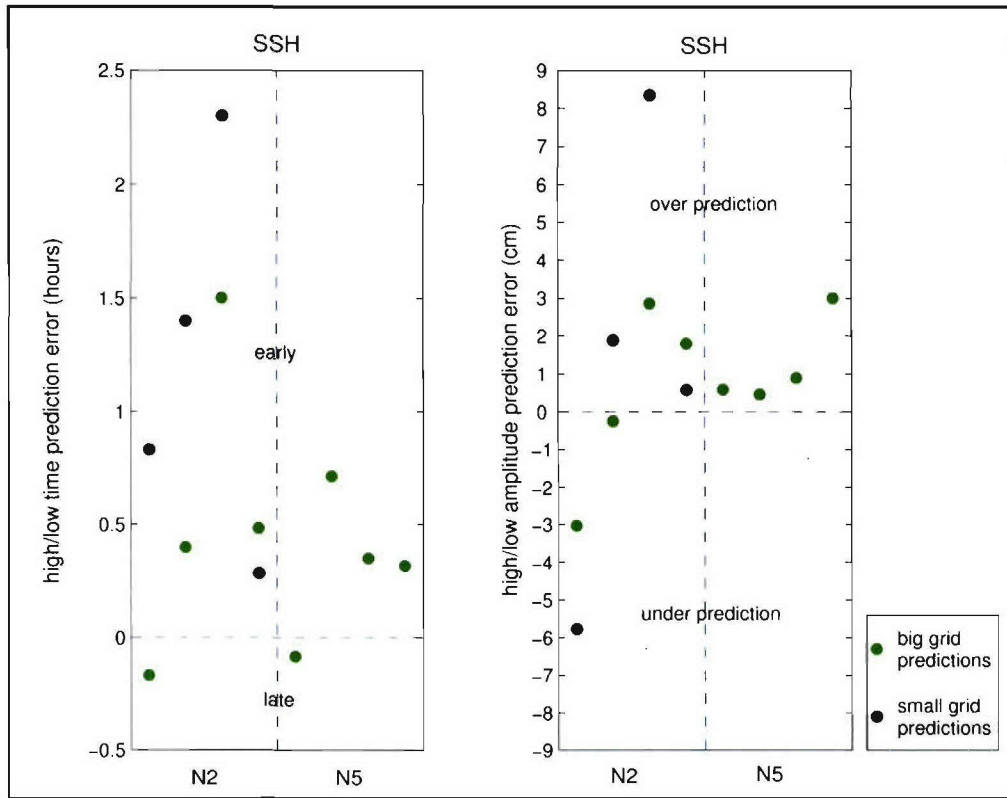
**Figure 9. LINKS Mooring N2 SSH Fluctuations**



**Note:** SSH fluctuations (blue line) projected from measured tidal coefficients at NRL LINKS mooring N5 (see figure 2). The green dots (big grid) are the predicted maximum and minimum points from the tabular output of PCTides simulations run inside NITES II. The small grid domain did not extend to N5.

**Figure 10. LINKS Mooring N5 SSH Fluctuations**

Figure 11 is a comparison of the predicted peak magnitudes and the times when the peak magnitudes occur. The former error is directly related to the PCTides-induced error in the MSL-to-MLLW offset correction. That is,  $\langle range_x \rangle$  from step 5 in figure 4 will not be perfectly estimated as shown by figures 9 and 10. Table 3 shows estimates of the additional error that would be induced in the MSL-to-MLLW offset correction for PCTides runs. The offset method error (TE from section 4.1.2.3) is large for stations N2 and N5 because they are both from the 11% of grid points with method percentage errors exceeding 10% (table 2). However, the error induced from PCTides inaccuracies is small (1% to 6%) for both test cases.



**Note:** The left panel gives the timing error (hours) with negative values indicating that the model lags the measurement values and positive indicating that the model leads the measurement values. The right panel gives the amplitude error (cm), with negative values indicating that the model under-predicts the magnitude (values less than measurement highs or more than measurement lows) and positive values indicating that the model over-predicts the magnitude.

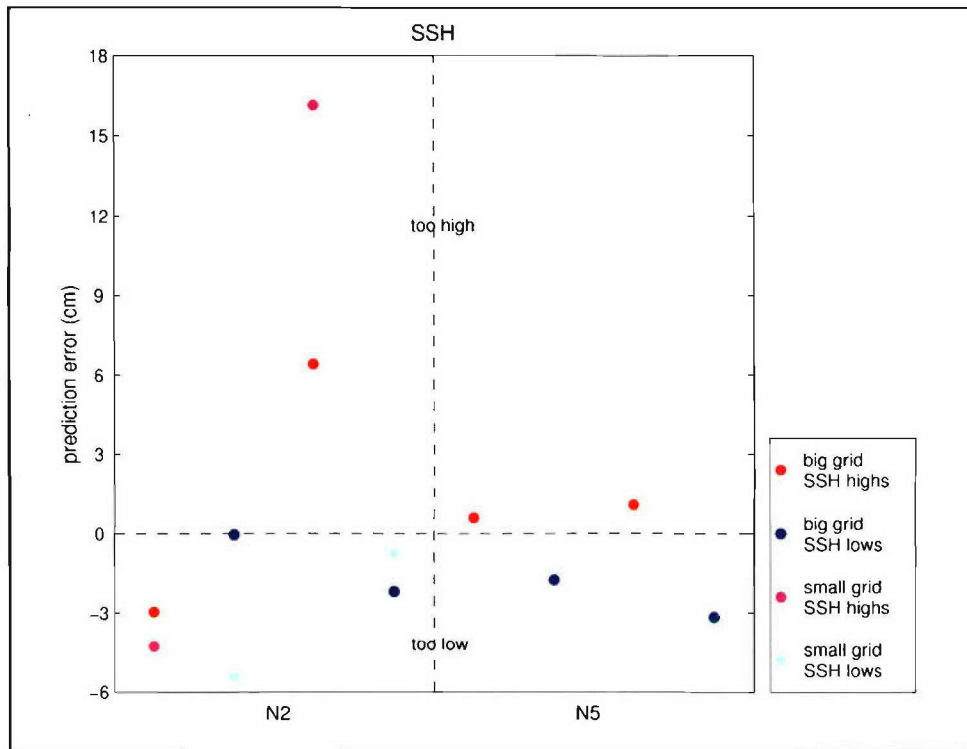
*Figure 11. PCTides Prediction Errors for SSH Highs and Lows in the KTS*

*Table 3. Estimated MLLW Offset Errors at LINKS Moorings N2 and N5, Accounting for PCTides Accuracy*

	Offset Method Error (cm)	Range Error (cm)	Induced Error (cm)	Induced Error (%)	Combined Error (cm)	Combined Error (%)
N2 Big PCTides Grid	3.9	-1.2	0.7	3	4.0	20
N2 Small PCTides Grid	3.9	0.3	0.2	1	3.9	20
N5 Big PCTides Grid	5.0	1.0	1.6	6	5.2	19



If a user of the NITES II system wants to know the tidal height at a particular time, both the amplitude and time error from figure 11 will contribute to a realized prediction error at the particular time. Combined errors (figure 12) were calculated for these tests using the times of highs and lows as reported by the model. They are simply the differences between the small and large grid predictions and the SSH for the same time reported in figures 9 and 10. Table 4 summarizes these error results. The percentage errors were normalized by the tidal range instead of the tidal signal at the predicted tidal peak time.



**Note:** The vertical axis values (cm) are the PCTides predictions minus the measurement SSH fluctuation at that particular time.

**Figure 12. Realized PCTides Prediction Errors at the Actual Times of Model-Predicted SSH Highs and Lows in the KTS**

**Table 4. SSH Prediction Errors at Times of Model Peaks Compared to MLLW Offset Errors in the KTS**

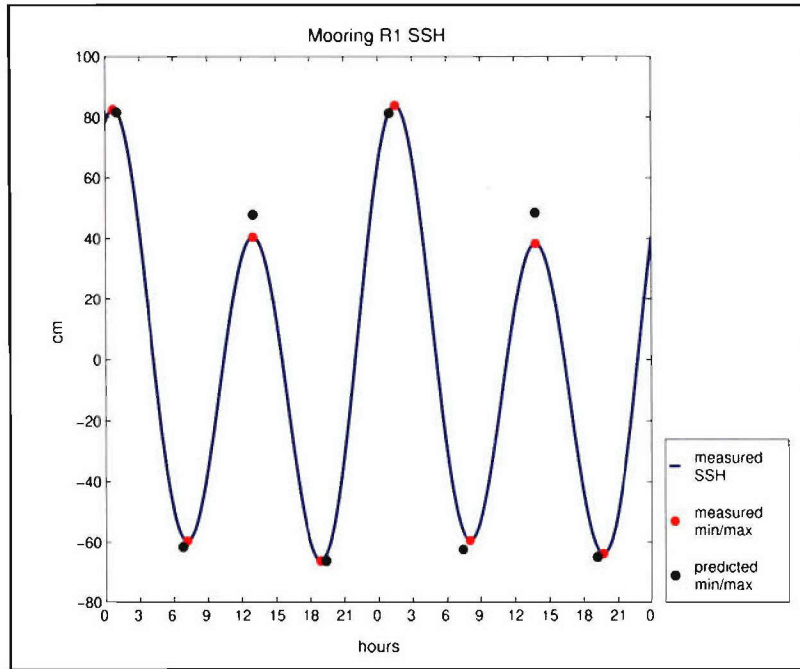
	Stations	Maximum SSH Error (cm)	Average SSH Error (cm)	Average SSH Error (%)	Combined Error (cm)	Average Total Error (ccm)
<b>Big PCTides Grid</b>	2	6.4	2.3	6	4.6	2.7
<b>Small PCTides Grid</b>	1	16.2	6.6	19	3.9	2.7

PCTides predictions from the big grid were more accurate at station N2 than for the small grid, despite a run with more than double the grid resolution. Prediction accuracy for the model is very sensitive to domain and grid selection. Although smaller domains can resolve coastal topography and bathymetry better, moving the edge boundary conditions closer to the coast can degrade predictions because the Grenoble global tidal model boundary conditions that force the model may have greater errors there. This is likely the cause of the poor SSH predictions at N2 for the small PCTides grid. However, despite this poor prediction for individual peaks and lows of SSH, PCTides actually predicts the tidal range at N2 better using the small grid than using the big grid (table 3). Thus, the induced error in the MLLW offset algorithm is lowest for this grid.

The average of the MSL-to-MLLW combined offset errors from table 3 are included in table 4 for comparison to the PCTides prediction errors. Because the offset errors are atypical for stations N2 and N5, the average offset method errors from table 2 are also listed. For this limited comparison, the MSL-to-MLLW offset errors are generally of the same order of magnitude as the average SSH anomaly prediction error. For the combined offset errors, stations N2 and N5 have anomalously high error because they are both located far away (43 and 94 km, respectively) from any IHO station. Although offset errors are sensitive to the distance from an IHO station (figure 7), PCTides prediction errors are not expected to be as sensitive to this parameter. Therefore, it is likely that the SSH errors found in table 4 are more generally representative of errors for the surrounding area than the offset errors would be. If it is true that the SSH prediction errors stay near the same level away from N2 and N5 and the offset errors drop to nearer their average (last column of table 4), then for much of the KTS the error for the offset correction would be similar (big grid) or smaller (small grid) than the error of PCTides SSH anomaly predictions.

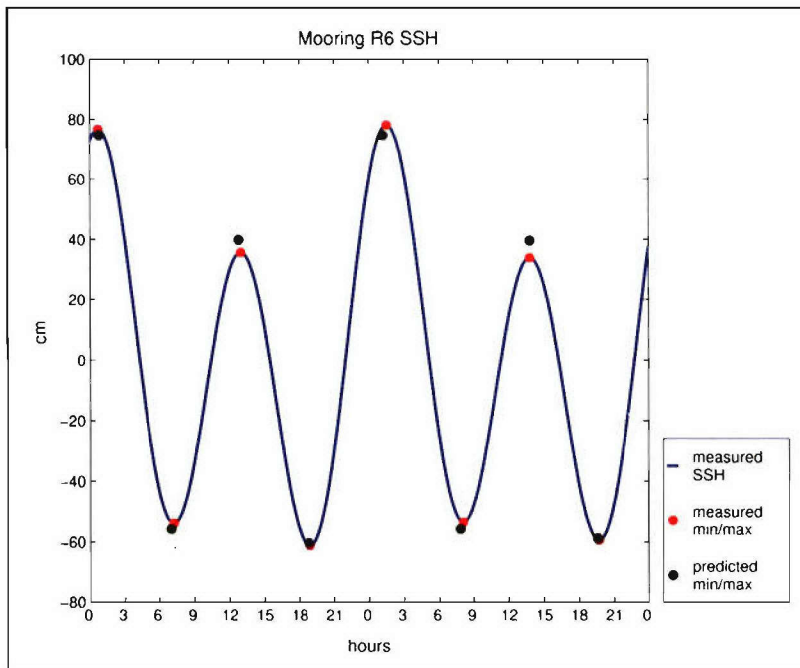
#### ***4.2.2 NJS Tidal Height Comparison Results***

Figures 13 and 14 show the tidal heights synthesized from measurements for the NJS (section 3.2.2.2) compared to the tabular output from the NITES II PCTides runs. The differences between the model and measurements were analyzed in the same manner as the differences for the KTS.



**Note:** SSH fluctuations (blue line) projected from measured tidal coefficients at NRL RAGS mooring R1 (see figure 3). The black dots are the predicted maximum and minimum points from the tabular output of PCTides simulations run inside NITES II.

**Figure 13. RAGS Mooring R1 SSH Fluctuations**

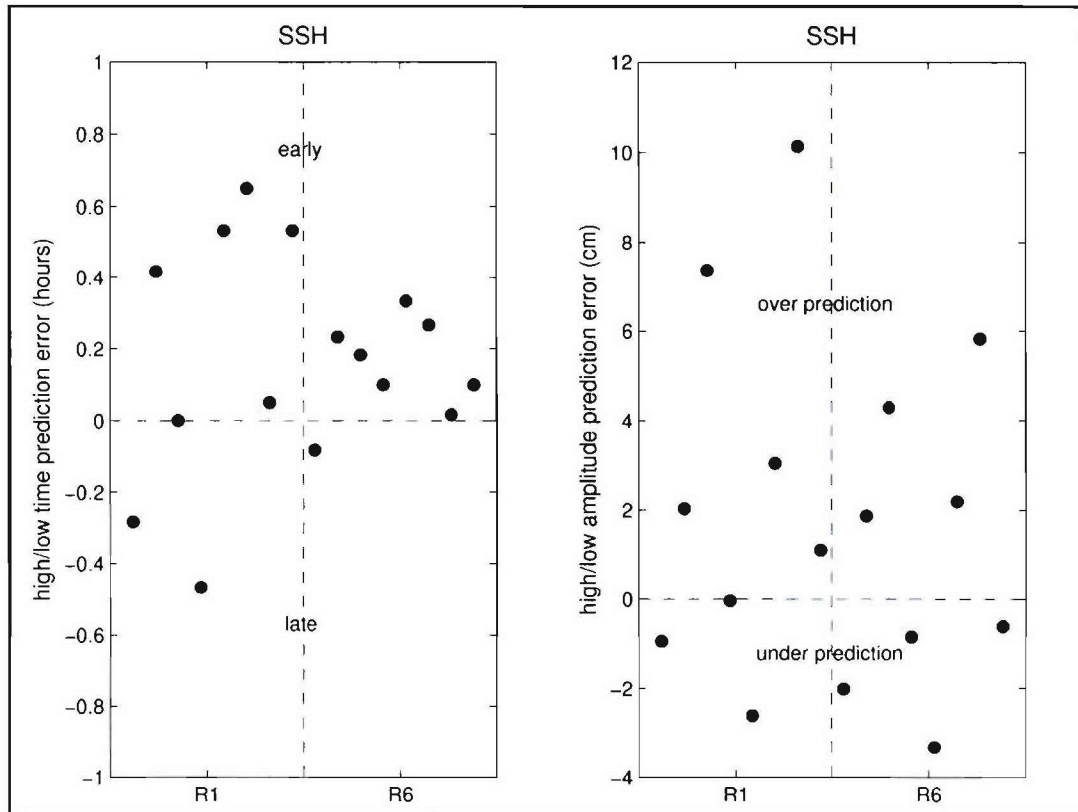


**Note:** SSH fluctuations (blue line) projected from measured tidal coefficients at NRL RAGS mooring R6 (see figure 3). The black dots are the predicted maximum and minimum points from the tabular output of PCTides simulations run inside NITES II.

**Figure 14. RAGS Mooring R6 SSH Fluctuations**



Figure 15 shows the timing and amplitude errors for PCTides predictions on the NJS. In general, timing errors are less than for the KTS and amplitude errors are slightly greater than for the KTS. However, because of greater signal amplitudes for the NJS comparisons, percentage errors are lower. Table 5 shows the mean predicted range errors and the magnitude of the MLLW offset determined from the measured tide coefficients.



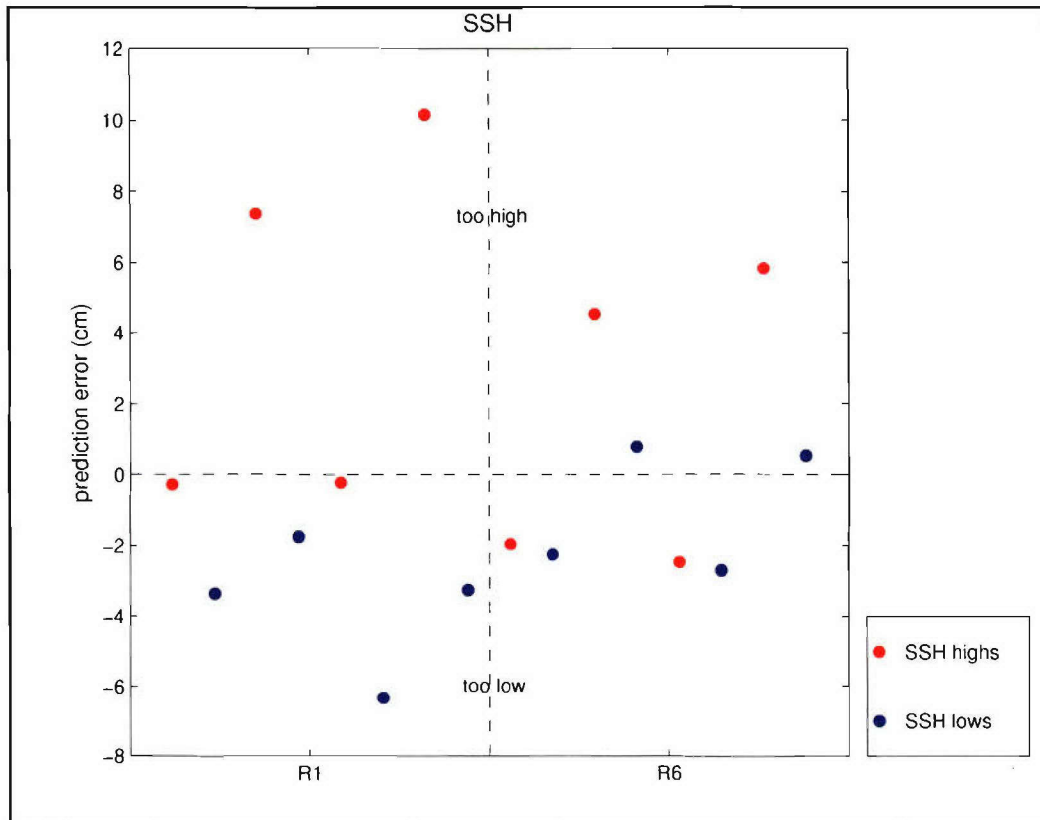
**Note:** The left panel gives the timing error (hours) with negative values indicating that the model lags the measurement values and positive values indicating that the model leads the measurement values. The right panel gives the amplitude error (cm) with negative values indicating that the model under-predicts the magnitude (values less than measurement highs or more than measurement lows) and positive values indicating that the model over-predicts the magnitude.

**Figure 15. PCTides Prediction Errors for SSH Highs and Lows on the NJS**

**Table 5. Range Errors and MLLW Offsets on the NJS**

	<b>Average Range (cm)</b>	<b>Range Error (cm)</b>	<b>Range Error (%)</b>	<b>MLLW Offset (cm)</b>
<b>R1</b>	148.3	1.2	0.8	-52.5
<b>R6</b>	137.7	3.4	2.5	-47.9

Figure 16 shows the realized prediction error that would occur at the times of the model-predicted SSH highs and lows. Errors are similar in magnitude to those found for the KTS. However, as discussed, percentage errors are lower because of greater tidal amplitudes. Table 6 presents the error statistics for these comparisons and the magnitude of the MLLW offset. The percentage errors were normalized by the average tidal range (table 5) instead of the tidal signal at the predicted tidal peak time.



**Note:** The vertical axis values (cm) are the PCTides predictions minus the measurement SSH fluctuation at that particular time.

**Figure 16. Realized PCTides Prediction Errors at the Actual Times of Model-Predicted SSH Highs and Lows on the NJS**

**Table 6. SSH Prediction Errors at Times of Model Peaks Compared to the Average MLLW Offset on the NJS**

	Stations	Maximum SSH Error (cm)	Average Magnitude SSH Error (cm)	Average Magnitude SSH Error (%)	Average MLLW Offset (cm)
<b>New Jersey Shelf</b>	2	10.1	3.4	2	-50

The PCTides run for the NJS is directly comparable to the PCTides run using the big grid for the KTS, as the domain size and grid spacing are roughly similar. Combining these limited comparisons, the average SSH errors were 2 to 3 cm, with maximum errors of 6 to 10 cm. The error values are similar for the two domains despite the differing geometries. This suggests that the errors reported in tables 4 and 6 are the level of SSH errors that should be expected from domains of these general sizes and spacings. These errors are well below typical MLLW offset values and are approximately equal to expected errors in calculating MLLW offsets using PCTides output.

## 5. SUMMARY

This study investigated algorithm development, implementation, and accuracy in converting MSL reference for sea surface heights (SSHs) currently used in the PCTides model to an MLLW reference. The changes recommended in section 6 can achieve this change in reference for PCTides SSH fluctuations.

Five algorithms were developed and tested for conversion from an MSL to an MLLW reference. The first algorithm was the MLLW offset calculator (section 3.1), which provided for near-exact reference conversion if tidal constituent data were available for a particular location. A second algorithm was developed for situations where tidal constituents were not available (e.g., PCTides prediction areas were distant from tidal stations). The MLLW offsets at the distant locations were determined by adjusting the MLLW offsets calculated from the closest, high-quality IHO station and applying the ratio of average ranges of the IHO and location time series (section 3.3):

$$MLLW_x = MLLW_{IHO} \cdot \frac{\langle range_x \rangle}{\langle range_{IHO} \rangle}.$$

Three similar algorithms were investigated that used LLW values instead of tidal range and/or average of ratios instead of ratios of average values.

Use of inverse range-weighting algorithms to consider multiple stations is deferred until IHO station selection algorithms are developed.

The ratio of average ranges algorithm (algorithm 4) performs well for the complicated tidal regimes present in the Korea/Tsushima Strait (KTS), capturing spatial changes in MLLW offset occurring at nearly a 100-km distance from IHO stations (section 4.1.1). Errors in the reference conversion can be quantified as errors specific to the way the algorithm approximates MLLW (method error) and errors caused by the use of imperfect data in the algorithm (induced error). The method error (with typical error amplitudes of 2.7 cm using 2-day time series in algorithm 4) proved to be less than 5% of the respective MLLW offset values for 75% of the locations in the KTS.

Range errors in PCTides predictions will produce an induced error in the MLLW reference offset for all algorithms that use time-series ranges to estimate offsets. Based on a limited comparison of PCTides SSH predictions and measurements in the KTS, the model is sufficiently accurate in tidal range estimates to achieve lower induced errors than method errors (section 4.2.1). Typical SSH anomaly prediction errors varied between 2 and 6 cm depending on the domain selection, with the larger domain run achieving higher accuracy, presumably due to better boundary conditions. Errors in SSH anomaly predictions were similar in magnitude to the typical total MLLW offset errors, and both were smaller than the magnitude of the MLLW offset

correction. Another limited comparison between model predictions and measurements on the New Jersey Shelf (NJS) confirmed that typical model prediction errors remained at less than 8 cm, independent of tidal range, and that these errors are much less than the MLLW offset correction (section 4.2.2).

Introducing an accurate MLLW reference change into the existing implementation of PCTides requires the output of IHO coefficient data, enhancements in IHO selection criteria, and an additional wind run by the model (section 4.1.2). The algorithm using the ratio of average ranges performed best for short PCTides runs (2 days), while the algorithm using the ratio of average LLW performed best for longer PCTides runs (29 days).



## 6. RECOMMENDATIONS

The authors recommend that the NITES II PCTides SSH reference be changed from MSL to MLLW for specific applications by applying a spatially dependent offset to the model, generated at run-time through implementation of the algorithm presented in this document. Specifically, the following tasks are necessary to achieve this goal in the near term:

- Adoption and implementation into the PCTides model code of the tidal analysis software of Pawlowicz, Beardsley, and Lentz (as modified by this study) and the MLLW calculator developed and evaluated in this study.
- Modification of model code inside PCTides to execute the steps of the MLLW offset algorithm of this study and to apply the offset to model output.
- Modification of PCTides model code to perform a background run without winds for purposes of MLLW offset calculation, in addition to any user-requested run with winds.
- Implementing PCTides to mandate model runs of at least 2 days duration.

Accuracy can be further improved over a broad range of environments by performing the following mid- to long-term tasks:

- Addition of IHO selection criteria to PCTides to select high-quality, long-duration stations from the set of stations available for a given area.
- Design and implementation of a “smart,” geographically-based IHO station selector.
- Design and implementation of a tool to support appropriate PCTides domain and grid size selection by nonexpert users.

## 7. REFERENCES

1. C. A. Blain, R. H. Preller, and A. P. Rivera, "Tidal Prediction Using the Advanced Circulation Model (ADCIRC) and a Relocatable PC-Based System," *Oceanography*, vol. 15, no. 1, 2002.
2. S. D. Hicks, R. L. Sillcox, C. R. Nichols, B. Via, and E. C. McCray, "Tide and Current Glossary," National Oceanic and Atmospheric Administration, National Ocean Service, Silver Spring, MD, 2000.
3. S. Gill and J. B. Schultz, eds., *Tidal Datums and Their Applications*, NOAA Special Publication NOS CO-OPS 1, National Oceanic and Atmospheric Administration, National Ocean Service, Silver Spring, MD, 2001.
4. "Data Base Description for Digital Bathymetric Data Base-Variable Resolution (DBDB-V) Version 4.2," Lockheed Martin, Manassas, VA, and Naval Oceanographic Office, Stennis Space Center, MS, 2002.
5. M. G. G. Foreman, "Manual for Tidal Heights Analysis and Prediction," Pacific Marine Science, Report 77-10, Institute of Ocean Science, Patricia Bay, Sidney, B.C., Canada, 1977.
6. R. B. Pawlowicz, B. Beardsley, and S. Lentz, "Classical Tidal Harmonic Analysis Including Error Estimates in MATLAB Using T\_TIDE," *Computers & Geosciences*, vol. 28, 2002, pp. 929-937.
7. J. W. Book, P. Pistek, H. Perkins, K. R. Thompson, W. J. Teague, G. A. Jacobs, M. S. Suk, K. I. Chang, J. C. Lee, and B. H. Choi, "Data Assimilation Modeling of the Barotropic Tides in the Korea/Tsushima Strait," *Journal of Oceanography*, vol. 60, 2004, pp. 977-993.
8. W. J. Teague, H. T. Perkins, G. A. Jacobs, J. W. Book, K. I. Chang, and M. S. Suk, "Low Frequency Current Observations in the Korea/Tsushima Strait," *Journal of Physical Oceanography*, vol. 32, 2002, pp. 1621-1641.
9. M. H. Orr, B. H. Pasewark, D. Walsh, P. Mignerey, J. Schindall, E. Carey, and M. McCord, "The Relationship of Array Gain to Shelf Break Fluid Processes: New Jersey Shelf—Winter Conditions, (in preparation), 2005.
10. B. H. Choi, "Digital Atlas for Neighboring Seas of Korean Peninsula," CD-ROM, Laboratory for Coastal and Ocean Dynamics Studies, Sung Kyun Kwan University, Seoul, Korea, 1999.

# APPENDIX

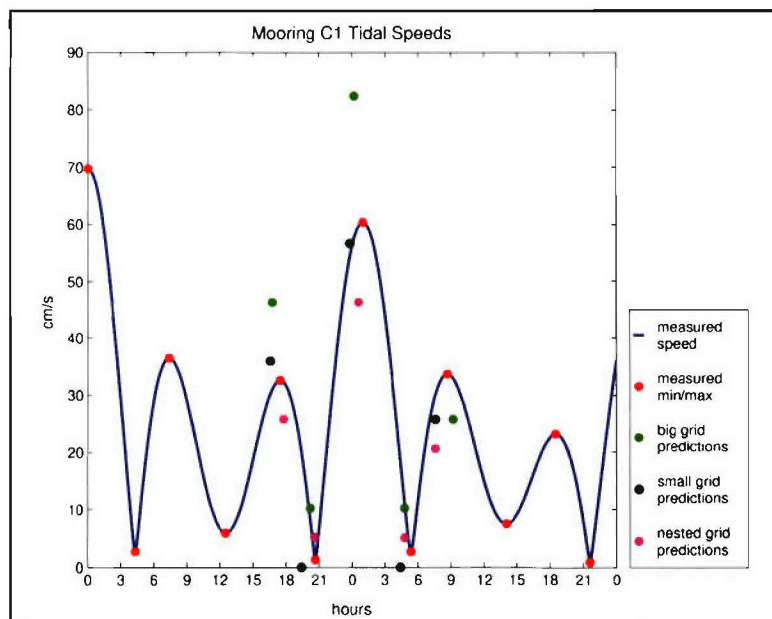
## RESULTS FROM LIMITED EVALUATIONS OF PCTides CURRENTS ACCURACY

### A.1 INTRODUCTION

PCTides predictions for tidal currents were compared to tidal currents synthesized from measurements. Although the accuracy of tidal current predictions does not have a direct impact on calculating MLLW offsets, this study was done to examine the overall accuracy of predictions and the issue of sensitivity to domain selection. Results of the comparisons from the Korea/Tsushima Strait (KTS) are presented in section A.2, and results of the comparisons on the New Jersey Shelf (NJS) are presented in section A.3. Section A.4 presents a summary.

### A.2 KTS TIDAL CURRENT COMPARISON RESULTS

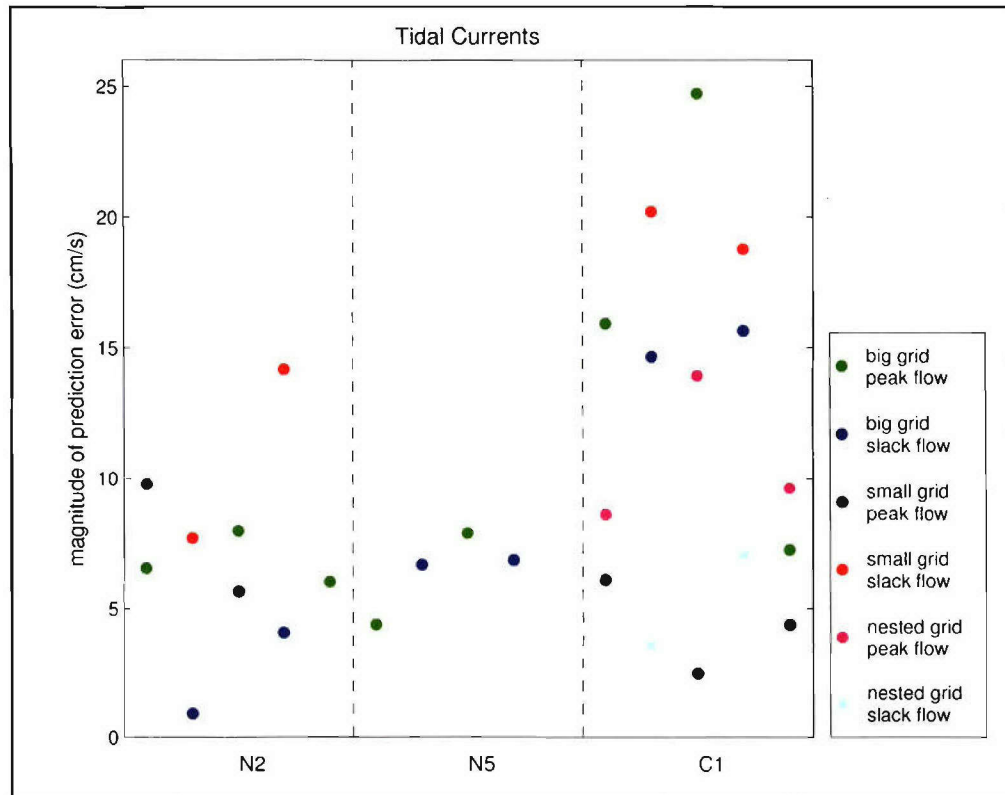
The setup for KTS current comparisons is explained in section 3.2.2.1. Comparisons were done for all three moorings (N2, N5, and C1). The tabular output from PCTides in NITES II reports tidal current speeds with the precision of 0.1 knot (5 cm/s). Therefore, errors on the order of 3 cm/s are expected simply from the lack of tidal speed precision. Figure A-1 shows the results from the C1 comparisons for all three domains: big, small, and nested grid. Predictions for this mooring in the 50-km-wide western channel of the KTS are improved by using the small or nested grid with 0.8-km grid spacing as compared to predictions using the big, 2.3-km grid.



**Note:** Tidal current speed fluctuations (blue line) projected from measured tidal coefficients at NRL LINKS mooring C1 (see figure 2). The green dots (big grid), the black dots (small grid), and the magenta dots (nested grid) are the predicted maximum and minimum speeds from the tabular output of PCTides simulations run inside NITES II.

*Figure A-1. LINKS Mooring C1 Tidal Speed*

Figure A-2 shows the comparison results for all the KTS moorings. To combine the errors associated with prediction errors in magnitude, timing, and current angle, a vector difference is computed between the predicted tides and the tides from measurements at the times of model-predicted peak and slack tidal currents. The values in figure A-2 are the magnitudes of the vector differences. Table A-1 summarizes the results from these comparisons. The percentage errors were normalized by the maximum tidal current speed rather than the tidal current signal at the predicted time.



**Note:** Magnitude (cm/s) of the vector difference between PCTides tidal current predictions and tidal currents projected from measurements in the KTS.

**Figure A-2. Realized PCTides Prediction Errors for Tidal Currents at Actual Times of Model-Predicted Peak and Slack Currents**

In this limited comparison, prediction accuracy is similar for the three grids, with average errors close to 9 cm/s. This is about 15% of the peak tidal current magnitude. The improvement from the big grid to the small grid for C1 predictions could be due to the increase in resolution in the model for this region of relatively complex features. Further improvement for the nested grid could be due to more accurate SSH boundary conditions (see section 4.2.1) that are brought to the small scale through the nesting. In the more open areas of the KTS represented by moorings N2 and N5, the predictions from the big grid have relatively low error. The increase in error for small grid predictions at N2, despite more than double the grid resolution, could also be due to the higher accuracy boundary conditions that can be obtained for the bigger domain extending further offshore.



**Table A-1. Tidal Current Prediction Errors at Times of Model Peak and Slack Tidal Currents for the KTS**

	<b>No. of Points and Stations</b>	<b>Maximum Error (cm/s)</b>	<b>Minimum Error (cm/s)</b>	<b>Average Error (cm/s)</b>	<b>Maximum Current (cm/s)</b>	<b>Average % Error (%)</b>
<b>N5 Big Grid</b>	4-1	7.9	4.4	6.5	37.9	17
<b>N2 Big Grid</b>	5-1	8.0	0.9	5.1	42.6	12
<b>C1 Big Grid</b>	5-1	24.7	7.2	15.6	60.4	26
<b>N2 Small Grid</b>	4-1	14.2	5.7	9.3	42.6	22
<b>C1 Small Grid</b>	5-1	20.2	2.5	10.4	60.4	17
<b>C1 Nested Grid</b>	5-1	13.9	3.6	8.6	60.4	14
<b>Big Grid</b>	14-3	24.7	0.9	9.3	60.4	18
<b>Small Grid</b>	9-2	20.2	2.5	9.9	60.4	19
<b>Nested Grid</b>	5-1	13.9	3.6	8.6	60.4	14

### **A.3 NJS TIDAL CURRENT COMPARISON RESULTS**

The setup for the NJS current comparisons is explained in section 3.2.2.2. The current measurements made at the mooring sites were of shorter duration than the pressure measurements. Therefore, the only tidal currents that were synthesized from the current measurements were from the O<sub>1</sub>, K<sub>1</sub>, M<sub>2</sub>, and S<sub>2</sub> tides. PCTides simulates Q<sub>1</sub>, P<sub>1</sub>, 2N<sub>2</sub>, N<sub>2</sub>, and K<sub>2</sub> tides in addition to the four tides resolved from measurements. These different sets of tidal coefficients could be responsible for some degree of mismatch between the model and data, especially with regard to P<sub>1</sub>, N<sub>2</sub>, and K<sub>2</sub>. A rough estimate of this constituent mismatch error\* is ±4 cm/s. However, the measured tides include the dominant M<sub>2</sub> tides, and energy from missing tidal constituents are at least partially carried into neighboring tides through the harmonic analysis.

Figure A-3 shows the comparisons for both mooring R1 and mooring R6.

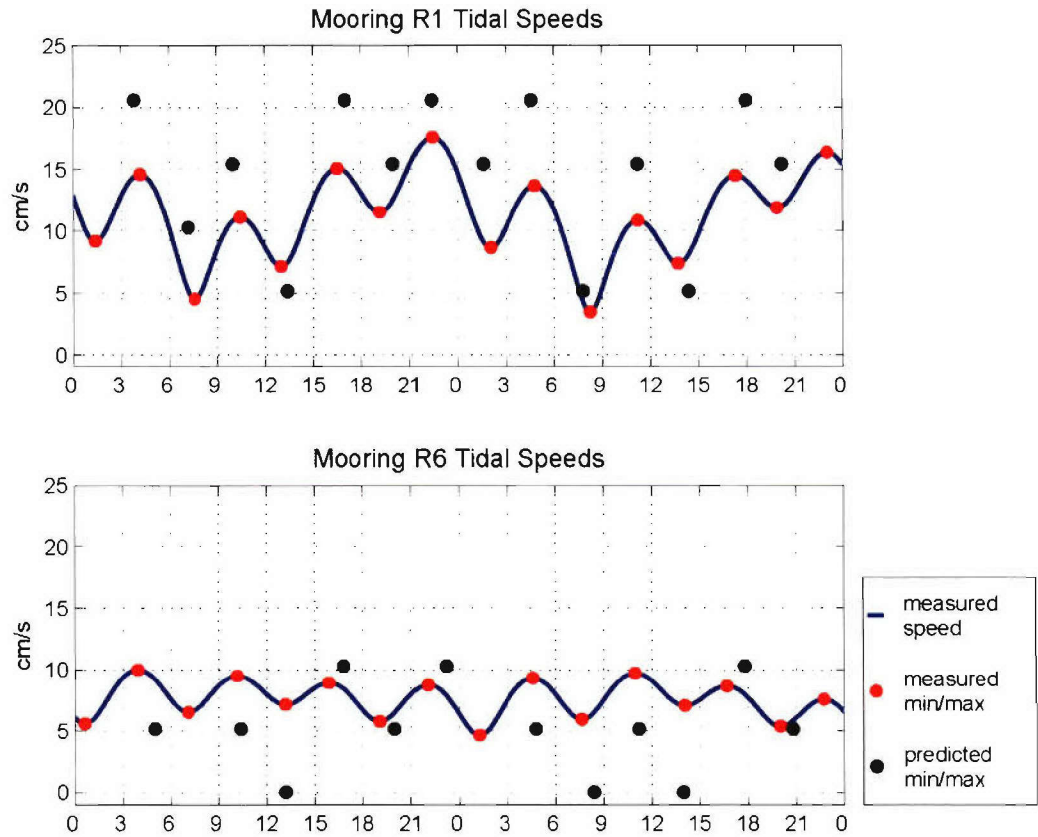
Table A-2 summarizes the current comparisons for the NJS. The percentage errors were normalized by the maximum tidal current speed instead of the tidal signal at the predicted time.

The average errors are above the level of error expected from the precision of the model reporting and the level of error expected from missing tidal coefficients. The percentage errors are high because of the low tidal current signal at these sites.

---

\*This is roughly based on the solutions from the four constituents and the equilibrium tidal potential.





**Note:** Tidal current speed fluctuations (blue line) projected from measured tidal coefficients at NRL RAGS (see figure 3) moorings R1 (top panel) and R6 (bottom panel). The black dots are the predicted maximum and minimum speeds from the tabular output of PCTides simulations run inside NITES II.

*Figure A-3. Tidal Speeds at RAGS Moorings*

*Table A-2. Tidal Current Prediction Errors at Times of Model Peak and Slack Tidal Currents on the NJS*

	No. of Points and Stations	Maximum Error (cm/s)	Minimum Error (cm/s)	Average Error (cm/s)	Maximum Current (cm/s)	Average % Error (%)
<b>R1</b>	14-1	12.1	2.5	8.0	17.6	46
<b>R6</b>	12-1	7.6	2.4	5.7	10.0	57
<b>NJS grid</b>	26-2	12.1	2.4	6.9	17.6	51

#### **A.4 TIDAL CURRENT COMPARISON SUMMARY**

Although the prediction difficulty was estimated to be less for the NJS region due to simpler coastlines and easier access to boundary conditions, the results for the limited current comparisons were similar to the results from the KTS. For grid resolutions of slightly more than 2 km (big KTS grid, NJS grid), the average magnitude of prediction errors ranged from 5 to 8 cm/s for all sites except for a 50-km-wide channel in site C1. These limited results suggest that this is the level of accuracy that should be expected for PCTides independent of the strength of the tidal currents.

Improving the grid resolution for the KTS simulations did not lead to an overall improvement in tidal current prediction for the sites considered. Doubling the resolution reduced errors for site C1, which is located in an area of complex topography and bathymetry, but errors increased for the more open site of N2. The average magnitude of prediction errors varied only slightly, between 7 and 10 cm/s, for various grid resolutions and two different ocean regions.

## INITIAL DISTRIBUTION LIST

<b>Addressee</b>	<b>No. of Copies</b>
NRL Stennis Space Center (J. W. Book)	6
Center for Naval Analyses	1
Defense Technical Information Center	2